

Accepted Manuscript

Alluvial to lacustrine sedimentation in an endorheic basin during the Mio-Pliocene:
The Toro Negro formation, central Andes of Argentina

Patricia L. Ciccioli, Sergio A. Marensi, William H. Amidon, Carlos O. Limarino,
Andrew Kylander-Clark



PII: S0895-9811(17)30519-9

DOI: [10.1016/j.jsames.2018.03.011](https://doi.org/10.1016/j.jsames.2018.03.011)

Reference: SAMES 1894

To appear in: *Journal of South American Earth Sciences*

Received Date: 12 December 2017

Revised Date: 15 March 2018

Accepted Date: 19 March 2018

Please cite this article as: Ciccioli, P.L., Marensi, S.A., Amidon, W.H., Limarino, C.O., Kylander-Clark, A., Alluvial to lacustrine sedimentation in an endorheic basin during the Mio-Pliocene: The Toro Negro formation, central Andes of Argentina, *Journal of South American Earth Sciences* (2018), doi: 10.1016/j.jsames.2018.03.011.

This is a PDF file of an unedited manuscript that has been accepted for publication. As a service to our customers we are providing this early version of the manuscript. The manuscript will undergo copyediting, typesetting, and review of the resulting proof before it is published in its final form. Please note that during the production process errors may be discovered which could affect the content, and all legal disclaimers that apply to the journal pertain.

**ALLUVIAL TO LACUSTRINE SEDIMENTATION IN AN ENDORHEIC BASIN
DURING THE MIO-PLIOCENE: THE TORO NEGRO FORMATION, CENTRAL
ANDES OF ARGENTINA.**

Patricia L. Ciccioli^{1,2}, Sergio A. Marensi^{1,2}, William H. Amidon³, Carlos O. Limarino^{1,2}
Andrew Kylander-Clark⁴

1. Universidad de Buenos Aires, Facultad de Ciencias Exactas y Naturales, Departamento de Ciencias Geológicas, Ciudad Universitaria, Pabellón 2, 1° piso, C1428EHA Buenos Aires, Argentina. ciccioli@gl.fcen.uba.ar , smarensi@hotmail.com , limar@gl.fcen.uba.ar
2. CONICET- Universidad de Buenos Aires. Instituto de Geociencias Básicas, Aplicadas y Ambientales de Buenos Aires (IGeBA), Argentina.
3. Geology Department, Middlebury College, Middlebury, VT, 05753, USA
wamidon@middlebury.edu
4. Earth Research Institute, University of California, Santa Barbara, CA, 93106, USA
kylander@geol.ucsb.edu

Corresponding author: Patricia L. Ciccioli ciccioli@gl.fcen.uba.ar

Departamento de Ciencias Geológicas, Facultad de Ciencias Exactas y Naturales,
Universidad de Buenos Aires. Pabellón 2, 1° piso, Ciudad Universitaria, C1428EHA
Buenos Aires, Argentina Tel: (54-11) 5285-8237; Fax: (54-11) 4576-3329

ABSTRACT

A 2400 meter-thick sedimentary column belonging to the Toro Negro Formation was recorded along the Quebrada del Yeso, Sierra de Los Colorados (Vinchina Basin), La Rioja province, NW Argentina. The Vinchina basin is a good example of a closed basin surrounded by the Precordillera fold and thrust belt to the west and basement-cored blocks to the north, south (Western Sierras Pampeanas) and east (Sierra de Famatina). Seven facies associations (FA) are described and interpreted to represent fluvial, lacustrine and alluvial environments developed in the southern part of the Vinchina basin from the Late Miocene until the earliest Pleistocene. The depositional evolution of the formation was divided in four phases. Phase I (~7-6.6 Ma) represents sedimentation in medial (FA I) to distal (FA II) parts of a southward directed distributive fluvial system with a retrogradational pattern. During phase II (6.6-6.1Ma), the distributive fluvial system was replaced by a mixed clastic-evaporitic shallow lake (FA III) in a high aggradational basin. In phase III (~6.1-5 Ma) the eastward progradation of a fluvial system (FA IV) was recorded as a distal clastic wedge. Finally, phase IV (~5-2.4Ma) records two depositional cycles of proximal clastic wedge progradation of fluvial-dominated piedmonts (FAV, FAVII) from the southwest (Sierra de Umango) and/or the west (Precordillera) with an intervening playa lake (FA VI).

Two new U-Pb ages obtained from zircons in volcanic ash layers confirm the Late Miocene age of the lower member of the Toro Negro Formation and permit a tight correlation with the central part of the basin (Quebrada de La Troya section). The sedimentation rate calculated for the dated lacustrine-fluvial interval is higher than the corresponding one in La Troya area suggesting a higher subsidence in the southern part of the basin.

During the Late Miocene (~7-6.6Ma) the ephemeral drainage was controlled by an arid to semiarid climate and initially dissipated mostly internally as terminal fan/distributive fluvial systems descending from the north. A thick lacustrine interval developed in the southern part of the basin between ~6.6 and 6.1 Ma during a period of high subsidence and closed drainage. Besides, this interval coincides with increased aridity recorded in other basins in the Northwest of Argentina. By ~6.1 Ma the area started to receive the first coarse-grained sediments heralding

the progradation of a clastic wedge from the southwest-west (Sierra de Umango and Precordillera) which fully developed during the rest of the Pliocene to the earliest Pleistocene (~5-2.4 Ma). The 6.1-2.4 Ma interval records ameliorating climate conditions.

Keywords: aridity- Late Miocene –distributive fluvial system - broken-foreland – Sierras Pampeanas

1. INTRODUCTION

Basin subsidence, uplift of source areas and climate are major controls on sedimentation in foreland basins isolated from the sea (“endorheic basins”). Furthermore, some studies suggest that relatively subtle tectonic activity along key drainage divides can also exert a first order cyclicity on facies distributions, especially lacustrine ones, due to changes on basin hydrology and geomorphology (e.g., Kowalewska and Cohen, 1998; May et al., 1999; Saéz et al., 1999; Carroll and Bohacs, 1999). Yet, few studies have documented the detailed relationship between specific tectonic events and the evolution of paleoenvironments in endorheic basins (Pietras et al., 2003; Pietras and Carroll, 2006; Saéz et al., 2007; Nichols, 2007; McKie, 2014).

Endorheic basins have good potential for preservation of distributive fluvial systems and lacustrine deposits (Saéz et al., 2007; Nichols, 2007; Cain and Mountney, 2009; Hartley et al., 2010; Weissmann et al., 2010; Weissmann et al., 2015). However, to preserve thick lacustrine successions the area of deposition must have a long history of relative base-level rise. This condition is met in underfilled closed basins (Bohacs et al., 2000). Relative sea level changes have no effects in endorheic basins and in a relatively arid climate any basin-center lake is likely to be relatively shallow (Nichols and Fisher, 2007). Fluctuations of only a few meters in the lake level may have little effect on the proximal and medial parts of the fluvial tract (Nichols and Fisher, 2007). Then, if there is enough subsidence and/or differential uplift at the basin margin the base-level in an endorheic basin will rise through time (Nichols, 2004), so the pattern of sedimentation will be aggradational/retrogradational. If not enough accommodation is created the pattern will be progradational. Recently, Weissmann et al. (2013) proposed a

conceptual model for prograding distributive fluvial systems which was quantified by Owen et al. (2017).

The Vinchina basin, located in the broken foreland of the Central Andes of Argentina (Fig. 1), seems to have had a complex evolution due to the interaction between the Precordillera fold and thrust belt and the Western Sierras Pampeanas and the Sierra de Famatina basement-cored blocks (Ciccioli et al., 2010a, 2011, 2013a; Ciccioli and Marensi, 2012; Marensi et al., 2015). The Vinchina and Toro Negro formations (Turner, 1964) exposed along the Sierra de los Colorados, La Rioja Province, Argentina (Fig. 2), make up the bulk of the sedimentary fill of the Vinchina basin. Altogether, they form one of the thickest Neogene sedimentary sequences related to the Andean Orogeny in northwestern Argentina having a composite thickness of more than 7.5 kilometers (Turner, 1964; Ramos, 1970; Ciccioli et al., 2011; Ciccioli et al., 2013b). A previous paleoenvironmental interpretation of the Toro Negro Formation (Ciccioli, 2008; Ciccioli and Marensi, 2012) suggested that its lower member (Ramos, 1970) presents a fining trend along depositional strike from conglomerates and gravelly sandstones deposited in broad alluvial plains in the north (Quebrada de Los Pozuelos section) to a thick sequence of fine-grained deposits in the south (Quebrada del Yeso section) (Fig. 2). Ciccioli et al. (2012) interpreted that the southern part of the basin was occupied mainly by an ephemeral mixed-clastic lake. The Sierra de Toro Negro in the north was the main source for this unit (Ciccioli et al., 2014). On the contrary, the upper member (Ramos, 1970) presents a coarser and more uniform lithology along the depositional strike recording a major change in the paleogeography of basin (Ciccioli, 2008; Ciccioli and Marensi, 2012; Ciccioli et al., 2014). This member records the progradation of the Precordillera thrust and fold belt from the west and the uplift of the Sierra de Umango in the south (Ciccioli et al., 2014). The ephemeral drainage was controlled by an arid to semiarid climate that prevailed during almost all the Mio-Pliocene (Ciccioli and Marensi, 2012; Marensi et al., 2015; Amidon et al., 2017).

Based on the absence of marine facies in the basin infill, and a lack of time-equivalent marine deposits in the surrounding areas (Reynolds et al., 1990; Malizia et al., 1995; Limarino et al., 2001; Tripaldi et al., 2001; Carrapa et al., 2008; Ciccioli et al., 2011; Ciccioli and

Marensi, 2012; Ciccioli et al., 2013b; Marensi et al., 2015), the Vinchina basin should be considered as endorheic or “mediterranean”. Therefore, eustatic variations cannot be invoked to explain changes in sedimentary depositional systems or cycles of erosion and deposition. Instead, other allogenic controls like regional tectonism, basin subsidence and climate should have controlled changes in accommodation and sediment supply. In this regard the evolution of the Vinchina basin can be compared with some of the well-known intermontane or “Laramide” basins in the Rocky Mountain region of the US (Dickinson, 1988) although the South American counterpart is still much less understood. For example, the Green River Formation of the great Green River Basin, in southwestern Wyoming, presents continuous exposures of lacustrine and associated alluvial strata allowing the identification, and direct correlation between lacustrine facies associations near the basin center and syntectonic alluvial strata deposited at the basin margin (Pietras et al., 2003; Pietras and Carroll, 2006) very much alike the Toro Negro Formation (Ciccioli and Marensi, 2012).

The age of the Toro Negro Formation has also been a matter of debate although all recent interpretations agreed in a Neogene age (Ciccioli et al., 2005; Amidon et al., 2016). Recently, Amidon et al. (2016) presented U-Pb ages from both volcanic tephra and detrital zircons collected from the Toro Negro Formation along the central (La Troya river) section improving age constraints on the pace of sedimentation and strengthening existing provenance interpretations (e.g. Ciccioli et al., 2014) but age correlation between the central section and the finer-grained southern area was not undertaken.

The aims of this paper are firstly to present a detailed facies description of the Toro Negro Formation along the Quebrada del Yeso (Fig. 2) interpreting the paleoenvironmental evolution of the southern part of the Vinchina basin. Especially, to analyze fluctuations on lake level over million years (progradation/retrogradation) and to relate them to changes in the foreland basin configuration. Second, to present two new U-Pb zircon ages from volcanic tephra cropping out along the Quebrada del Yeso correlating them with those reported by Amidon et al. (2016) for the type section along the La Troya river. In addition these new data permit to estimate a

sedimentation rate in a closed basin (endorheic) and to relate the sedimentary record to the Late Miocene- Pliocene episodes of greater aridity.

2. GEOLOGICAL SETTING

The study area is located in the Central Andes of Argentina (27° to 33° S) encompassing from west to east the Main Cordillera, the Cordillera Frontal, the Precordillera, the Sierras Pampeanas and the Famatina System (Fig. 1). This segment is characterized by low-angle subduction of the Nazca Plate (Ramos et al., 2002) that converges at an oblique angle with respect to the South American Plate, producing a complex deformation pattern including some degree of strike-slip movement (Rossello et al., 1996; Introcaso and Ruiz, 2001; Japas et al., 2016). In this area several foreland basins were formed during the Cenozoic including the Vinchina Basin (28° and 29° S). This basin was bounded to the west by a thin-skinned thrust-belt (Precordillera), to the east by an emerging upland area that forms the present-day Sierra de Famatina (Famatina System) and to the north and south by basement-cored blocks (Sierras de Toro Negro and Umango–Espinal, respectively, Fig. 1).

The Toro Negro Formation (Turner, 1964) was originally divided into two members (Ramos, 1970). The lower member is composed mainly of sandstones, mudstones, muddy intra-formational breccias and extra-formational conglomerates with some tuff layers. These rocks were deposited in different types of anastomosing fluvial systems, braided rivers, siliciclastic and saline shallow lakes, as well as minor fluvial-eolian interaction systems (Ciccioli and Marensi, 2012). For the most part, sedimentation took place under semiarid to arid climatic conditions indicated by abundant desiccation cracks and intercalations of eolian-fluvial interaction deposits. The upper member is mainly composed of cobble conglomerate and coarse-grained sandstones deposited in braided rivers and streamflow-dominated piedmonts with some intercalations of fine-grained sediments corresponding to a tuffaceous playa-lake (Ciccioli and Marensi, 2012). In the central (Quebrada de La Troya section) and northern (Quebrada de Los Pozuelos section) parts of the basin the unit was further subdivided into three depositional sequences (DSs of Ciccioli et al., 2010b; Ciccioli et al., 2014). The lower member

is split between DSI and II while the upper member is equivalent to DSIII. The base of all sequences are demarcated by erosional unconformities, which may record periods of regional base-level change (Ciccioli and Marensi, 2012; Ciccioli et al., 2014). The basal unconformity at the base of DSI has the highest relief, including a paleovalley carved into the underlying Vinchina Formation, which causes DSI to be ~25% thicker at north (Los Pozuelos) where it fills the valley (Limarino et al., 2010). DSII become considerably coarser in the La Troya section and record alluvial gravels prograding from north to south in an underfilled basin (Ciccioli and Marensi, 2012). DSIII is composed of thick successions of clast-supported conglomerates and coarse-grained sandstones deposited in piedmont and proximal braided plains, alternating with comparatively thin intervals dominated by mudstones, fine-grained tuffs and tuffaceous deposits (Ciccioli, 2008; Ciccioli and Marensi, 2012).

Ciccioli et al. (2014) used detrital modes of sandstones and conglomerate clast composition to interpret sediment provenance areas for the Toro Negro Formation. They concluded that the Sierra de Toro Negro (to the north) and the Cordillera Frontal and Precordillera (to the west) were the main sources for DS I and II (lower member of the Toro Negro Formation). On the contrary DS III (upper member) recorded a progressive increase in the supply from the eastern Precordillera (to the west) with additional material from the Sierra de Umango to the south. Evidences of synchronic volcanism were recorded in the DS I, the upper part of DS II and the lower part of DS III. These conclusions were also supported by U-Pb ages of detrital zircons (Amidon et al., 2016).

Age estimates for the Toro Negro Formation have ranged from Plio-Pleistocene (Reynolds, 1987, Tabbutt et al., 1989, Ré and Barredo, 1993), to late Miocene-early Pliocene (Ciccioli et al., 2005). Recently, Amidon et al. (2016) presented eight U-Pb zircon ages from volcanic tephra from the La Troya section refining the age of the Toro Negro Formation to approximately 6.87 to 2.37 Ma (Late Miocene-earliest Pleistocene).

3. METHODOLOGY

A detail section of the Toro Negro Formation was measured along the Quebrada del Yeso (Fig. 2). Facies associations are described using lithofacies (Table 1), architectural elements (Table 2) and boundary surfaces (Fig. 3) following Miall's (1996) code with modifications.

U-Pb ages of zircons collected from tephra were used for age determination and correlation to the La Troya section (Fig. 2). Two tuff beds were found along the stratigraphic section, located with GPS coordinates and sampled. The poorly consolidated tuffs were mildly crushed in the lab until sand-size using a ball mill and then panned to concentrate heavy minerals. Magnetic components were separated using a hand-size magnet and then zircons were selected and hand-picked under the microscope. To further purify zircons, the samples were then etched for one hour with concentrated HF/HNO₃ (2:1 ratio) at room temperature. Zircons were then mounted in epoxy, and polished parallel to the c-axis for analysis by laser ablation inductively coupled plasma mass spectrometry (LA-ICPMS). Zircon analyses were performed at the UCSB LASS facility using a Photon Machines Analyte 193-nm excimer laser and Nu Instruments Plasma MC-ICPMS, following the methods described in Kylander-Clark et al. (2013). Analyses targeted the rims of zircons free of cracks or inclusions using a spot size of 30 μ m and a repetition rate of 4 Hz. Results were standardized using the 91500 zircon reference material (Wiedenbeck et al., 1995). Standards GJ1 (601.7 ± 1.3 Ma; Jackson et al., 2004) and Plesovice (337 ± 0.37 Ma; Sláma et al., 2008) were used for secondary quality control, yielding mean $^{206}\text{Pb}/^{238}\text{U}$ ages of 599.3 ± 4.5 (n=22; MSWD = 1.4) and 337.9 ± 3.6 Ma (n=27; MSWD = 1.1). All tephra ages are based on $^{206}\text{Pb}/^{238}\text{U}$ ages corrected for initial Pb and secular disequilibrium. The initial Pb correction uses ISOPLOT (Ludwig, 1991), and assumes a common $^{207}\text{Pb}/^{206}\text{Pb}$ ratio of 0.84 (Stacey and Kramers, 1975). The secular disequilibrium correction follows Schaerer (1984) and assumes a Th/U ratio of 3.2 based on an average value of Mio-Pliocene ignimbrites in the Incapillo region.

4. FACIES ASSOCIATIONS

The sedimentology of the Toro Negro Formation in the southern part of the Vinchina Basin was recorded from a 2400 meters-thick single section measured along the Quebrada del Yeso

(Fig. 4). A lower fine-grained (mudstone-sandstone) section 1590 meters thick corresponds to the lower member of the unit and an upper coarse-grained (conglomerate-sandstone dominated) interval 810 meters thick represents the upper member of the formation.

The lower member presents a fining-coarsening upward (sand-clock) trend, with the lower fining-upward part much thicker than the upper coarsening-upward section. The upper member is built up by the overlapping of two lenticular units that pinch out towards the north. Lenses are more than 1 km wide and up to 500 m thick. Internally the first unit shows a fining upward trend from conglomerate-dominated facies into sandstone/mudstone-dominated facies while the second one only exposes the basal conglomerate-rich facies association and is unconformably covered by Pleistocene deposits.

Within the lower and upper members, seven facies associations (FA) were identified and interpreted to represent deposition in ephemeral mixed lake and alluvial-fluvial systems. The sedimentological descriptions and interpretations of each facies associations and depositional systems are summarized in Figure 5 and Table 3 discussed in detail below.

4.1 FA I: shallow sandy river

4.1.1 Description.

This 342 meter-thick unit constitutes the lowermost part of the Toro Negro Formation along the Quebrada del Yeso (Fig. 4). This facies association is composed of lenticular beds (0.5 to 1 meter-thick) bounded by slightly erosive basal (order 5th) and convex-up top surfaces forming the CHm element (Fig. 6a, b). Internally they are made by lenticular beds up to 0.5 meters-thick (single channels, CHs, Fig. 6b) bounded by erosive basal surfaces (4b) evidenced by thin muddy partitions occasionally associated with gypsum laminites (El) and convolute stratification. Within channels, medium-grained sandstones with low-angle stratification (Sl) or horizontal stratification (Sh) with parting lineation (Shp) and heterolithic sandstone-mudstone lamination (She) conform the SB element. Trough (St) and planar (Sp) cross-stratified sandstones are very rare or absent. Occasionally, ripple cross-laminated sandstones (Sr) are present in the upper part of these deposits and asymmetric ripples are preserved at the top of

these beds. Low-angle third-order (3) surfaces corresponding to lateral migration of channels (LA element) are only sporadically recognized.

Tabular beds up to 3 meters-thick of reddish, massive (Fm) and dotted mudstones (Fd) and ripple cross-laminated (Sr) and heterolithic laminated (She) fine-grained sandstones and mudstones compose the FF element of the floodplain deposits. Mudstones are frequently intensely bioturbated (Fig. 6c). Medium- to fine-grained ripple cross-laminated (Sr), heterolithic laminated (She) or massive (Sm) sandstones intercalate within the FF deposits forming 20 to 50 cm thick lenticular to tabular beds bounded by planar basal surfaces (order 4c). They are interpreted as crevasse splay deposits (CS element).

Sandy channel deposits (CHm, CHs, SB) and muddy and sandy floodplain deposits (FF, CS) form in occasions up to 4 meters-thick coarsening-upward cycles (Fig. 6a).

4.1.2 Interpretation

This unit is interpreted as a shallow sandy fluvial system dominated by lens-shaped channels (CHm) flowing over a sandy to mixed sand-mud floodplain deposits (FF and CS, Fig. 5). Facies distribution suggests that deposition took place within fixed channels isolated in the floodplain. Channels remained stationary until completely filled by single or multiple flood events and only then they avulsed to an adjacent part of the floodplain. This behavior has been interpreted to represent strongly confined channels in low to middle sinuosity (sporadic LA) multichannel rivers likely to anastomosing. An alternative could be to interpret an incipient fluvial system represented by channel belts with poor development in both lateral extension and depth.

Shallow channels are mostly represented by sandy mesoforms (SB) with upper-flow regime sedimentary structures (Shp) that migrate during flash floods due to an ephemeral regime (Foley, 1978; Reid and Frostick, 1987; Mather, 2007). Gypsum laminites associated to reactivation surfaces (order 4b) as well as deformational structures could be indicating sudden and episodic deposition followed by desiccation periods. Each flood event was separated by short periods when evaporites formed in hypersaline shallow waters (Picard and High, 1973).

Floodplain deposits are dominated by fine-grained sediments (FF) as well as by the progradation of sandy crevasse deposits (CS). The first ones are related to subtle pedogenic processes indicating short episodes of subaerial exposure while crevasse deposits are frequently bioturbated by invertebrates. The progradation of the crevasse deposits over the fine-grained floodplain sediments generate stratigraphically transitional avulsion (cf. Jones and Hajek, 2007) by aggradation- and progradation-denominated heterolithic avulsion deposits (c.f. Krauss and Wells, 1999).

4.2 FA II: Distal sheetflow-dominated DFS

4.2.1 Description

This facies association (192 m thick) sharply covers FAI and develops up to 10 meter thick coarsening-upward cycles (Fig. 6d, e). A thin (less than 0.8 m-thick) white tabular tuff layer appearing at the top of this unit was sampled (TN 43, Fig. 6g) and dated (see section 5). This tephra level has physical continuity to the north for more than 25 kilometers.

Parallel (Fl) mudstones, ripple cross-laminated (Fr) reddish siltstones and white gypsum laminites (El) interlaminated in centimeter- to millimeter-scale tabular beds are the dominant lithology (Fig. 6f). Occasionally, massive mudstones and siltstones (Fm) associated to dotted fine-grained sandstones (Sm) conform the distal terminal splay element (SHd). Other kinds of deposits are fine- to medium-grained ripple cross-laminated sandstones (Sr) in thin lobate beds bounded by planar basal surfaces and wavy tops, and tabular beds of ripple cross-laminated (Sr) to massive (Sm) sandstones (Fig. 6f). These deposits correspond to the proximal terminal splay element (SHp).

Seldom, lenticular to lensoid beds (from 0.2 to 1 m thick) of medium- to coarse-grained sandstones bounded by slightly erosive basal surfaces (order 4c) marked by levels of pebbly-sandstone (SGm) or fine-grained conglomerates (Gm) are recognized. Above these lag deposits there are parallel (Sh) and ripple cross-laminated (Sr) sandstones. These rocks form the CHs element. In some cases, desiccation cracks and abundant invertebrate traces are present.

4.2.2 Interpretation

This unit is interpreted as the distal part of a sheetflow-dominated distributive fluvial system (Hampton and Horton, 2007; Weissmann et al., 2010; Hartley et al., 2010; Fig. 5) composed of shallow and ephemeral channels that prograded into a shallow waterbody (FA III below), similar to that described by Kelly and Olsen (1993) and discussed by North and Warwick (2007).

Tabular beds of interlaminated mudstones, siltstones and gypsum correspond to the basin (i.e. playa-lake) where fine-grained sediments settled down from suspension alternated with precipitation of gypsum from sulphate-saturated brines. Massive and dotted sandstones are product of bioturbation and pedogenesis (Retallack, 2001).

Distributive fluvial systems are composed of lenticular and tabular to sheet sandstones. The former are interpreted as shallow distributive channels (CHs) while the latter correspond to the proximal (SHp) to distal (SHd) terminal splays from these channel over the alluvial plain or playa-lake (Fisher et al., 2007; Nichols and Fisher, 2007; Hampton and Horton, 2007; Fisher et al., 2008; Cain and Mountney, 2009). Coarsening-upward cycles suggest episodic progradation of a sheet flow-dominated distributive fluvial system over a saline mud flat (Cain and Mountney, 2009; Weissmann et al. 2013).

4.3 FA III: ephemeral lake

4.3.1 Description

This 740 m- thick unit transitionally covers AF II and is dominated by tabular beds of interlaminated reddish mudstones, siltstones, whitish gypsum and scarce fine-grained sandstones and gray limestones (Fig. 7a). Very thin tabular beds of mudstones and siltstones present parallel (Fl) to ripple cross (Fr) lamination and interlamination with gypsum laminites (El) composed of fibrous crystals with chevron fabric (Fig. 7b,c,d). Coarsening-upward arrangements 10 cm-thick from heterolithic (flaser, She) to massive (Sm) or ripple cross-laminated (Sr) sandstones at the top are frequently developed. Desiccation cracks of different sizes are common. Lobe-shaped beds (2 to 15 cm- thick), bounded by planar basal and wavy or

convex-up top surfaces, of ripple cross-laminated (Sr) and massive (Sm) sandstones are intercalated in the former lithology (SHd). Different types of small-scale ripples (symmetrical, symmetrical with devastated crest, asymmetrical with sinuous- and linguoid-crests) are usually preserved at the top of these sandstone beds (Fig. 7e). Lenticular beds (up to 0.50 m-thick) of greenish brown medium-grained sandstones with parallel-lamination (Sh), parting lineation (Shp) and sometimes with antidunes (Sa) and deformational structures appear occasionally (SHp).

Limestones (L) are commonly present in tabular beds (up to 0.20 m thick) and are grain-supported ooids-dominated (90%) with 10% of equant sparry cement (calcite). These Oosparites (Folk, 1962) are made up mainly of surficial and spherical ooids with micritised or terrigenous cores (Fig. 7f). Scarce long ooids likely correspond to skeletal grains (bivalve shells) that suffered oolitization and replacement of the original shell structure. Some bivalve shells with their original structure preserved are found.

The above mentioned rocks form up to 20 meters coarsening-upward arrangements.

Near the top of this unit there is a tephra layer which has physical continuity to the north for more than 25 kilometers. This layer was sampled and dated in the Quebrada de La Troya area by Amidon et al. (2016) yielding an age of 6.11 Ma (sample Ash 6).

4.3.2 Interpretation

This facies association is interpreted as an ephemeral, shallow, lacustrine system dominated by saline mudflat deposits (Hardie et al., 1978, Handford, 1982; Fig. 5). Mud-sized clastic sediment was supplied to the lake center by ephemeral (poorly channelized) sheet flows. The presence of crystalline and laminated gypsum interlaminated with mudstones indicates shallow and hypersaline waters (Hardie et al., 1978, Tucker, 1991, Yechieli and Wood, 2002; Warren, 2016). These deposits formed in the central part of the lake (saline mud flat to salt pan) by evaporative pumping during the driest periods with low-water levels (Arenas and Pardo, 1999). Desiccation cracks further indicate subaerial exposures and drying out of muddy sediments. Common interbedding of evaporite and mudstone layers suggests intermittent

periods of flooding, freshening, and sediment advection from the surrounding lake plain, followed by evaporative concentration.

On the other hand, the oolitic limestones formed at times of significant freshwater inflow (Arenas and Pardo, 1999). The dominance of superficial oolites indicates shallow agitated waters (Strasser, 1986) suggesting lake marginal deposits (Gierlowski-Kordesch, 2010).

During periods of lake level highstands, channels of the fluvial systems flowed into a shallow body of water forming a series of deltaic lobes or terminal splays (Fisher et al., 2007; Saéz et al., 2007). The low gradient basin floor and partly confined nature of inflowing rivers are thought to be responsible for the deposition of sheets under higher-flow regime conditions and/or terminal splays (SHp; Nichols and Fisher, 2007; Hampton and Horton, 2007; Fisher et al., 2008). They are interpreted as sand flats. Mudstones and heterolithic deposits represent the most distal facies (SHd: distal terminal splay). Abundant wave symmetrical ripples in some deposits highlights the importance of wave action as a post-depositional reworking mechanism in these systems. In this setting the small-scale coarsening upward cycles represent expansions of the lake during periods of high water inflow by surficial runoff (Fig. 7b, c).

The repetitive coarsening-upward intervals of marginal facies (sandy-mud flat) over central facies (saline mud flat-salt pan) deposits are interpreted to record contraction-expansion cycles of the water body.

4.4 FA IV: low-sinuosity multichannel rivers

4.4.1 Description

This facies association (318 m-thick) makes up the upper part of the lower member of the Toro Negro Formation at Quebrada del Yeso section transitionally covering FA III (Fig. 4).

Tabular beds up to 4 m-thick of reddish brown mudstones corresponding to the FF architectural element are dominant (60%). Mudstones and siltstones show parallel (Fl) and ripple cross-laminations (Fr) with thin intercalation (2 to 10 cm-thick) of greenish massive (Sm) to ripple cross-laminated (Sr) fine-grained sandstones (Fig. 8a,b). In occasions, thin crystalline

gypsum laminites (El) are also present (Fig. 8c). A distinguish feature is the presence of massive mudstones (Fm) with spheroidal concretions and small coaly wood remains (Fig. 8d). Tabular to sheet beds (10 to 50 cm thick) of massive (Sm) to ripple cross-laminated (Sr) medium-grained sandstones appear in a subordinated proportion. They are bounded by planar basal surfaces (order 4c) and constitute crevasse splay elements (CS).

Ribbon to lentiform beds, 1 to 3 m-thick, with slightly erosive basal surfaces of coarse-grained to pebbly sandstones (SGm) with occasional fine- to medium-grained (Gm) conglomerates and some oversized clasts form multi-storey channel belts (CHm, Fig. 8a, e) (40%). Simple channels up to 0.50 m-thick form lenticular to tabular beds separated by erosive surfaces (4b). They are floored by a thin deposit of massive fine- to medium-grained conglomerates (Gm), followed by crude planar cross-stratified (Gp) to massive (Gm) fine-grained conglomerates and pebbly-sandstones (SGm) defining the GB element (Fig. 8e). Conglomerates are matrix-supported (sandy matrix) and polymictic with subrounded clasts (5 cm to 15 cm length) of high-grade metamorphites and granites and few low-grade metamorphites (Fig. 8e). These deposits alternate with low-angle (Sl) to horizontal (Sh) stratified medium-grained sandstones frequently culminating with ripple cross-laminated (Sr) sandstones conforming the dominant SB element.

A whitish tuff layer (1.5 m thick) was recognized in the middle part of this facies association. This tuff level is massive at the base but shows a diffuse horizontal stratification (Fig. 8f). It was sampled (TN 10/07) and dated (see Section 5).

4.4.2 Interpretation

This FA is interpreted as a low-sinuosity multichannel river with sandy to mixed sand-gravel channels, encapsulated into fine-grained floodplain deposits (FF; Fig. 5). Due to the predominance of these fine-grained deposits, this system is similar to the rapid aggradation proposed by Makaske et al. (2002) and affected by volcanoclastic supply episodes.

Channels were dominated by the migration of pebbly to sandy (pebbly-sands to gravels) dunes and, occasionally by low-relief transversal bars (SB>GB) that migrated under lower-flow

regime condition. Sporadically, these conditions changed due to large volume of volcanoclastic material generating hyperconcentrated flood-flows (Smith, 1986). These flow deposits are characterized by massive to diffuse stratification (Fig. 8f) that could represent rapid fluvial aggradation generated by drowning of the streams due to the high supply of tephra (Vessell and Davies, 1981; Smith, 1986, 1987a, 1987b).

The higher proportion of floodplain deposits than channel deposits is a clear sign of the high aggradation rate of this system (Fig. 8a). Aggradation due to sheetfloods with low development of thin crevasse splay deposits predominated in the floodplain. Channels could have suffered occasional abrupt avulsions (Jones and Hajek, 2007).

Floodplain deposits present signs of subtle paleoclimatic variations. The dominance of reddish mudstones with intercalations of thin gypsum laminites (Fig. 8c) indicates an overall semiarid climate. However, reddish massive mudstones with spheroidal concretions and coalified wood remains evidence pedogenic process and more humid conditions (Fig. 8d). Although poorly developed paleosols are common in semiarid conditions, the presence of woody-coal may suggest short-lived episodes of wetter climate (Retallack, 2001).

4.5 FA V: *Streamflow-dominated piedmont*

4.5.1 *Description*

This unit appears twice in the section forming the base of the lower and upper lenses. The first time is 330 meters thick and unconformably covers FA IV, representing the base of the upper member at Quebrada del Yeso area (Fig. 4). The second time is 160 meters thick, sharply covers FA VII and constitutes the top of the Toro Negro Formation along the Sierra de Los Colorados (Fig. 4). It is made up of medium- to coarse-grained conglomerates (75%), minor coarse- to medium-grained pebbly sandstones and scarce mudstones arranged in finning upward cycles. Sandstones and mudstones occasionally constitute up to 25% of the unit when measured off the lens axis.

Tabular beds of gray conglomerates up to 15 m thick presenting low-relief erosive bases (5e) represent composite channel belts (CHm; Fig. 9A). Internally they are made by lenticular

beds up to 1 m thick of clast-supported (sandy matrix) medium- to coarse-grained conglomerates (clasts up to 30 cm in diameter) conforming the GB element (Fig. 9A). They are massive (Gm) or show clast imbrication (Gi) in the lower levels grading upward into either low-angle cross (Gl) stratification and parallel stratification (Gh) or alternatively tabular (Gp) and trough (Gt) cross stratification. Sometimes small lenses (20 cm wide and 10 cm thick) of massive pebbly sandstones (SGm) are preserved at the top. Lenses of massive matrix-supported (sandy matrix) conglomerates (Gmm) corresponding to the SG element are rarely present. Clast composition shows two lithologic associations. The first one (greenish) is composed of volcanic, sedimentary rock fragments, granites, and low amount of high-grade metamorphic rock fragments (Fig. 9B). The second one (grayish) is dominated by high-metamorphic fragments and white granites (Fig. 9C) with minor proportion of volcanic, green low-metamorphic and sedimentary fragments.

Sheet or wedge-shaped beds of massive (Sm) or ripple cross-laminated (Sr), medium- to fine-grained sandstones and siltstones (Fm/Fr) correspond to the SO element. Reddish massive siltstones (Fm) and fine-grained sandstones (Sm) show abundant root marks, iron stain, infrequently thin gypsum laminae (El) and centimeter-thick green tuffs.

4.5.2 Interpretation

A streamflow-dominated piedmont (Smith, 2000) is interpreted for this unit (Fig. 5). These systems form alluvial slopes of roughly parallel stream channels lacking the morphology of alluvial fans. They commonly develop on low-angle piedmonts with predominance of channelized flows instead of sheet flows (Smith, 2000).

The high proportion of conglomerate facies with well-developed gravel bars (GB element) and rare occurrence of hyperconcentrated flows (SG) suggest that this FA represents deposition by gravel-bedload streams. Fine-grained facies include sandy interchannel deposits (SO) with indication of well-developed vegetation and heterolithic sand-silt floodplain deposits with infrequently evaporites and ash fall deposits. Development of vegetation is common in

water saturated interchannel sands as well as in hydromorphic floodplains (Slate et al., 1996; Retallack, 2001).

4.6 FA VI: sandy-muddy tuffaceous playa-lake

4.6.1 Description

This lenticular unit composed by sandstones and mudstones with minor conglomerates is up to 190 meters-thick and conformably covers FA V in a sharp transition. Tabular, fine-grained deposits (elements SHp, SHd and FF, 70%) predominate over channelized coarse-grained ones (CHs and CHm, 30%). Both of them form coarsening and thickening up arrangements up to 15 meters thick (Fig. 9D).

Tabular beds up to 10 m thick of fine-grained red ripple-cross (Sr)- or parallel-laminated (Sh) sandstones and massive mudstones (Fm) conform elements SHd (>50%) and FF (<40%). Lenticular to lobe-shaped beds up to 0.25 m thick correspond to occasional (<10%) proximal terminal splay (SHd). They have plane bases (4c surfaces) and convex up tops and are made up of medium-to coarse-grained sandstones with occasional granules. They present a thin basal lag of granules and massive, coarse-grained sandstones (SGm) covered by medium-grained massive (Sm), parallel (Sh) or ripple cross-laminated (Sr) sandstones. The presence of fine-grained tuffaceous material is noteworthy. They form tabular beds that can be laterally continuous for several hundred meters to a few kilometers or lenticular beds up to 0.5 m thick. The former presents planar or slightly erosive bases (4b surfaces) sometimes blanketed with a centimeter-thick intraformational breccia (Bi) and followed by fine-grained tuffaceous sandstones showing tabular low angle cross-bedding (Sl), parallel (Sh) and convolute bedding (Sc).

Lenticular beds 0.5 to 2 m thick and 5 m wide ($w/d < 15$) with erosive basal surfaces (4b) represent the channel architectural element (CHs). They are composed by gray massive conglomerates with some clast imbrication (Gm/Gi) followed by tabular- (Gp), low-angle (Gl) cross-bedded or horizontal (Gh) stratification. In occasions individual channels pile up forming two to three stories lenticular channel belts (CHm) up to 6 m thick. They present planar to

slightly erosive basal surfaces (5a). Conglomerates are coarse- to medium-grained (8 to 20 cm in diameter), clast-supported (sandy matrix) and dominated by volcanic rocks fragments with minor amounts of metamorphic and sedimentary rocks and granites.

4.6.2 Interpretation

This FA represents deposition in a mixed sandy-muddy tuffaceous playa-lake associated with ribbon shallow gravely channels (Bentham et al., 1993; Kelly and Olsen, 1993; Miall, 1996; Hampton and Horton, 2007; Nichols and Fisher, 2007) (Fig. 5).

Largely dominant fine-grained tabular deposits (SHd>>FF) developing coarsening up cycles represent the distal part of a progradational distributive fluvial system in a high-subsidence and high-aggradation setting. Tabular sandstone sheets are interpreted to represent deposition associated with unconfined flow just downslope of confined channels. In this respect, sheets are interpreted as downslope terminal splays (SHp).

Channels were relatively fixed and shallow (CHs, CHm). Poorly confined lenticular channel deposits are the result of either single or multiple flood events in which channels scoured a single broad erosional surface in underlying fine-grained deposits. Sporadic occurrences of gravel lithofacies (Gi, Gl and Gp) suggest that the development and migration of gravel bars occurred but it was not a dominant mechanism.

The relatively fixed shallow channels with thick sandy floodplain deposits seem to be similar to the medial to distal part of a distributive fluvial system (Nichols and Fisher, 2007; Weissmann et al., 2010; Hartley et al., 2010) or alternatively the middle part of a sheet flow-dominated distributive fluvial system (Hampton and Horton, 2007). A prominent feature of the distal zones in the distributive fluvial model is that much more sandstone is present as sheet deposits than as channel-fill facies (Nichols and Fisher, 2007; Weissmann et al., 2013). These sheets have sharp, sometimes erosive base and this scouring at the base of the sheets suggest local channelization of flow. Isolated sheets may occur, but they are mostly found in packages of laterally extensive units. Thick-bedded muddy and silty facies between the sheet sandstone beds show evidences of paleosol development (Retallack, 2001).

4.7 FA VII: gravel-bed braided river

4.7.1 Description.

In the study area this lenticular unit, with a maximum thickness of 100 meters, appears encased within the upper third of FA VI. It is mainly composed of medium- to coarse-grained gray conglomerates and coarse-grained sandstones (75%) and medium to fine-grained sandstones and occasional mudstones and siltstones (25%) arranged in fining-upward cycles (Fig. 9E).

Lenticular beds from 2.5 to 13 m-thick, several meters up to few tens of meters wide with basal erosive surfaces (5e) form the composite channel element (CHm). They are made up by amalgamated lenticular gravelly beds up to 3 m-thick and few meters wide, floored by erosional surfaces (4b) constituting individual channels (CHs). The thicker channel belts show less amalgamation and the preservation of sandy interbeds. Internally, coarse- to medium-grained conglomerates with clasts up to 50 cm in diameter present three main lithofacies arrangements. The first one shows clast-supported massive conglomerates (Gm) passing upwards into large-scale (up to 2 m-thick) tabular (Gp) or trough cross-stratification (Gt) and finally into low-angle or parallel-stratified (Gh) conglomerates (GB). Centimeter-thick beds of coarse- to medium-grained massive (Sm) or low-angle (Sl) cross-stratified sandstones are common on top of the former probably representing poorly developed or relicts of the SB element. The second type is composed of clast- to matrix-supported (sandy matrix) medium- to fine-grained conglomerates with occasional outsized clasts. They are massive (Gm) or show a diffuse parallel (Gh) stratification (GB). Finally, lenticular beds with planar basal surfaces (4b) of massive matrix-supported (Gmm) fine- to medium-grained conglomerates (clasts up to 5 cm in diameter) make up the SG element. Conglomerates are polymictic with subrounded to subangular clasts of granites, volcanic rocks, red sandstones and high-grade metamorphic rocks.

Tabular beds (0.3 to 4 meter-thick) of medium-grained sandstones with diffuse ripple-cross (Sr), parallel lamination (Sh) or massive (Sm) due to bioturbation represent the SO element (80%). Massive (Fm) to diffuse ripple-cross laminated (Fr) siltstones and mudstones

associated with thin gypsum laminites (El), desiccation cracks, vertical burrows, rizoliths or mottled textures make up the FF element (20%).

4.7.2. Interpretation

This facies association represents deposits of a deep, gravel-bed braided system similar to that described by Miall (1996) with the floodplain dominated by sandy sheet-flow deposits. In channel deposits (CHm) mainly correspond to the development of gravel bars and bedforms (GB). Channels were deep allowing for the migration of thick longitudinal to transverse and linguoid bars with well-developed slip faces. During low-water stages thin lenses or wedges of sandy lithofacies (SB) were deposited at bar margins due to run off, or on lee surfaces and in channels during waning flows. Occasional sediment gravity flows deposited massive matrix supported gravels which inter-finger into water-laid longitudinal to linguoid bars deposits.

Deposition in the floodplain resulted in sandy (SO) to finer-grained (FF) facies associated with overbank flooding resulting from unconfined flow originating from overtopped channels; or alternatively downslope, unconfined sedimentation associated with terminal flooding stages. The presence of vegetation (pedogenesis) indicated by the rizoliths and mottled structures (Retallack, 2001), anchors the fine-grained sediments and results in fair preservation potential. Preservation of floodplain deposits suggests high subsidence rates associated to rapid aggradation (Bentham et al., 1993; Bristow et al., 1999).

Overall this FA is interpreted to represent the proximal to medial areas of a distributive fluvial system (Kelly and Olsen, 1993; Hampton and Horton, 2007; Nichols and Fisher, 2007; Weissmann et al., 2013). The coarsest deposits occurring in the deepest channels are found in the proximal zones of the system. These are sandy or conglomeratic facies showing clast imbrication, cross-bedding and preservation of bar structures indicating that they are the deposits of braided streams close to margin of the basin.

5. NEW U/PB AGES AND CORRELATION WITH LA TROYA RIVER AREA

Recently, Amidon et al. (2016) reported six tephra ages ranging from 6.87 to 4.95 Ma for the lower member of the Toro Negro Formation along the central (La Troya) section (Figs. 2). One of their tuff layers (Ash-6) has lateral physical continuity between the Quebrada de La Troya and Quebrada del Yeso, with an eruptive age of 6.11 My. The two new tephra ages from samples collected along the Quebrada del Yeso yielded ages of 6.64 ± 0.1 Ma (TN 43) and 5.40 ± 0.12 Ma (TN 10/07) respectively (Fig. 10 and Table S1), indicating that sedimentation took place during Messinian times and corroborating the Late Miocene age for the lower member of the Toro Negro Formation.

The sedimentation rate calculated from undecompressed sediments between samples TN 43 and TN 10/07 is about 0.80 mm/yr and is slightly higher than the sedimentation rate (0.65 mm/yr and 0.5 mm/yr) for the same interval along the Quebrada de La Troya (recalculated from data of Amidon et al. (2016) and calculated by Ciccioli et al. (2017) by magnetostratigraphy). These values may be representing mean sedimentation rates between a lower interval of higher subsidence (lacustrine/playa-lake interval) and an upper one of lower accumulation towards the top of the lower member as indicated by Amidon et al. (2016). The sedimentation rate for the lacustrine interval can be calculated using the age of 6.64 Ma of the sample TN 43 which lies almost at the top of FA II and the age 6.11 Ma of sample Ash 6 of Amidon et al. (2016) which is in the transition between FA III and IV (Fig. 11). According with this the 740 meters-thick lacustrine interval in the southern part of the basin was deposited between 6.64 and 6.11 Ma yielding a rate close to 1.4 mm/yr. In addition, the sedimentation rate for a 100 meter-thick interval of lacustrine deposits along the Quebrada de La Troya can be constrained using samples Ash 5 and Ash 6 of Amidon et al. (2016) and is of 1.25 mm/yr.

The age of TN 43 (6.64 ± 0.1 Ma) is close to the estimated younger ages of detrital zircons in sample V11 (~ 6.6 Ma) and certainly older than Ash 5 (6.19 ± 0.10 Ma) of Amidon et al. (2016) suggesting that these samples correspond to the same depositional interval (Fig. 11). TN 43 is located near the top of the 192 meters-thick FA II interpreted as the medial to distal part of a distributive fluvial system. In the La Troya area sample V11 was collected within a 170 meters-thick interval (FA VI of Ciccioli and Marenssi, 2012) composed of gravely-sandy

braided channels encased into sandy to muddy interchannel areas interpreted as the proximal parts of a distributive fluvial system or the toe of a fluvial-dominated piedmont. In addition, sandstone compositions at the Quebrada del Yeso also show synchronous changes with the proximal Quebrada de La Troya section belonging to the plutonic-metamorphic petrofacies and the distal ones (Quebrada del Yeso) to the mixed petrofacies defined by Ciccioli et al. (2014). This correlation strengthens previous interpretations based on facies distributions and sandstone composition of a strong north to south gradient with a main source area located to the north/northwest (Ciccioli and Marensi, 2012; Ciccioli et al., 2014).

The age and stratigraphic position of TN 10/07 (5.40 ± 0.12 Ma) reported herein coincides with that of sample Ash 8 (5.46 ± 0.03 Ma) of Amidon et al. (2016) strongly suggesting that both samples correspond to the same ash layer (Fig. 11). TN 10/07 is located in the upper part of FA IV close to the top of the lower member of the Toro Negro Formation. This 318 meter thick unit represents deposition in a fluvial setting with low-sinuosity mixed sandy-gravelly channels encased into sandy-dominated floodplain deposits. In the La Troya area Ash 8 was collected from a 310 meters-thick interval (AF VII of Ciccioli and Marensi, 2012) composed of shallow, low-sinuosity sandy-gravelly channels with wide interchannel areas interpreted as the medial to proximal parts of a distributive fluvial system or fluvial fan (Ciccioli and Marensi, 2012). This correlation suggests that similar paleoenvironments evolved in both areas and therefore suggesting the absence of any N-S gradient in facies distribution. This fact is also supported for the homogeneous composition of sandstones and gravels that indicate mixed provenance from high-grade metamorphic (Sierras Pampeanas basement), volcanic (Cordillera Frontal) and low-grade metamorphic (Precordillera) sources (Ciccioli et al., 2014).

6. EVOLUTIONARY MODEL

The lower member of the Toro Negro Formation in the southern part of the basin (i.e. Quebrada del Yeso) shows important differences relative to the central (Quebrada de La Troya) and northern (Quebrada de Los Pozuelos) sections (Ciccioli and Marensi, 2012). Overall it is finer-grained, resulting in a clear trend from coarser to finer facies from north to south along

depositional strike much like the upper part of the underlying Vinchina Formation (Marenssi et al., 2015). In contrast, the uppermost part of this member and the upper member of the Toro Negro Formation do not follow this rule, showing fairly homogenous coarser-grained facies along depositional strike.

Four phases are recognized in the evolution of the Toro Negro Formation in the Quebrada del Yeso (Fig. 12).

6.1 Phase I (~7-6.6 Ma): DFS from the north

In the lower part of the lower member the upsection changes from thick lenticular sandstone units (FA I) to relatively thin tabular sandstone/mudstone units (FA II) and finally into muddy dominated thin-bedded deposits with thin gypsum and limestones intercalations (FA III). This indicates a gradual transition between confined flows in shallow channels to unconfined flows in sheets and finally into an ephemeral lake, similar to the depositional model proposed by Hampton and Horton (2007) for ephemeral sheetflow-dominated distributary fluvial systems. The overall fining upward trend suggests a retrogradational pattern due to increased accommodation. Centimeter and meter-scale cycles within each depositional system may attest to autocyclic processes, shorter progradational pulses or both. Distributive fluvial systems can be present in both endorheic (internally drained) and exorheic (externally drained) aggradational basins in a wide range of climatic settings (Weissmann et al., 2010; Hartley et al., 2010). In our case, the distributive fluvial system was developed in an endhoreic basin which ephemeral floods, desiccation cracks, poorly developed paleosols and evaporites attest to arid to semiarid conditions with an ephemeral lake (FA III) as type termination (Fig. 12). Generally, in this type of basin water losses through evapo-transpiration exceed the input from direct precipitation and rivers entering the basin (Nichols and Fisher, 2007). However, an upland area which has a much higher precipitation is needed because a moderate supply of water is required to establish and maintain the rivers of the distributive system (Nichols and Fisher, 2007). On the other hand, if an excess of water is supplied to an endorheic basin a lake will develop and the river system will feed a small scale lake delta (Nichols and Fisher, 2007; Nichols, 2007). According to

previous studies in the Vinchina basin (Ciccioli and Marensi, 2012; Ciccioli et al., 2014) we envisage an elevated area located proximal to the north (Sierra de Toro Negro) and another one more distally to the west (Precordillera and Frontal Cordillera) during deposition of the lower part of the lower member of the Toro Negro.

6.2 Phase II (~6.6-6.1Ma): Ephemeral lake

This stage began to 6.6 Ma (TN43) and continues to ~6.1 Ma according to the tephra layer (Ash 6) dated in the La Troya by Amidon et al. (2016). The existence of an ephemeral lacustrine system (FA III) in the middle part of the lower member in the southern part of the basin also suggests a closed drainage and an underfilled setting (Carroll and Bohacs, 1999). Gypsum beds and limestones indicate shallow hypersaline waters and high evaporation regime, while the lack of eolian deposits in the area may suggest a relatively high water table. These deposits associated to ephemeral floods and desiccation cracks attest to continue arid to semiarid conditions. Besides, this interval coincides with the latest Miocene increased aridity event recorded in several basins of Northwest Argentina as Iglesias, Angastaco, Huaco (i.e. Starck and Antózegui, 2001; Ruskin and Jordan, 2007; Bywater-Reyes et al., 2010; Amidon et al., 2017). In particular, Amidon et al. (2017) associated this interval of enhanced aridity to a period of slower erosion.

The paleogeography of the basin was similar to phase I although an incipient elevated area was probably located to the south-southwest (Sierras de Umango-Espinal) acting as a basin spill-point or low topographic barrier (Fig. 12). This basement didn't act as a supply area but it collaborated to the high subsidence. So, this thick lacustrine interval (FA III) was developed at or around ~6.6 Ma to 6.1 Ma in a period of accelerated subsidence (~1.4 mm/yr at this section and 1.25mm/yr at Quebrada de La Troya according to Amidon et al. (2016)) during which basin isolation allowed for a shallow mixed clastic-evaporitic lake to develop in the southern part of the basin.

6.3 Phase III (~6.1-5 Ma): Distal clastic wedge from the W-SW

After this episode of ephemeral lacustrine sedimentation (FA III) the upper part of the lower member from ~6.1 to 5 Ma (latest Miocene to earliest Pliocene) records the progradation of fluvial systems (FA IV) into more distal positions in the basin. This change in sedimentation is marked by a progressive increase in sand content and the arrival of coarse-grained sediments. This influx of sediments progressively decreases the accommodation vs sediment supply rate. As there is no evidence of contemporaneous incised valleys in the basin this shift may be accomplished by a reduction in basin subsidence, a marginal tectonic uplift or a climate change. During this phase subtle indicators of more humid conditions as the preservation of small coalified wood remains are recorded. Indeed, a shift into a more humid climate may increase the surficial runoff and the amount of sediment transported into the basin by fluvial currents. The increase in the grain size and the change to multi-storey, coarse-grained bodies indicate higher energy hydrodynamic conditions possibly related to a regional climate change with more humid conditions (or at least more water availability) potentially linked to a tectonic event bringing coarser-grained sediment into the basin. Similar more humid conditions are also recorded in the NW Argentina and in other parts of the south hemisphere for latest Miocene to Pliocene (Starck and Anzótegui, 2001; Hynek et al., 2012; Sniderman et al., 2016; Amidon et al., 2017). Interestingly sandstone and conglomerate clast compositions began to show a significant participation of low-grade metamorphic fragments derived from the Precordillera added up to high-grade metamorphic fragments and granites from crystalline basement. In addition, a more homogeneous N-S facies distribution also suggests that this unit heralds the progradation of a clastic wedge from the west recording a pulse of uplift in Precordillera. But the high-grade metamorphic fragments evidence also the distal progradation of a clastic wedge from the emergent Sierra de Umango in the southwest (Fig. 12).

6.4 Phase IV (~5-2.4Ma): Proximal clastic wedge from the W-SW

The upper member records a major change in basin configuration. Its base is a low-relief erosional unconformity and the conglomerate clast-composition of the basal FA V confirms the change in the source area. Based on detrital modes of sandstones and conglomerate clast-

compositions Ciccioli et al. (2014) interpreted a pulse of uplift in the Cordillera Frontal and Precordillera and the Sierra de Umango to the west-southwest. Therefore, the initial coarse-grained deposits (FA V) are thought to represent a syntectonic low-angle piedmont, likely prograding from the west and/or southwest. The subsequent FA VI and FA VII both correspond to medial/distal to proximal areas of a new distributive fluvial system developed in a closed basin. The sharp basal contact of the finer-grained FA VI and the return of the high-grade metamorphic clast petrofacies in the conglomerates of both FA VI and VII (Ciccioli et al., 2014) suggest that this system was sourced from a basement-cored area, the Sierra de Umango to the southwest (Fig. 12). Finally, a new episode of uplift in the Precordillera and the development of another piedmont from the west are indicated by the last recurrence of FA V.

7. CONCLUSIONS

Along the Quebrada del Yeso, the Toro Negro Formation is represented by a 2400 thick sedimentary column which was divided in four phases. Phase I (~7-6.6 Ma) represent sedimentation in medial (FA I) to distal (FA II) parts of a southward directed distributive fluvial system. During phase II (~6.6-6.1 Ma), the distributive fluvial system was replaced by a mixed clastic-evaporitic shallow lake (FA III). Then, in the phase III (~6.1-5 Ma) the progradation of a fluvial system (FA IV) was recorded as a distal clastic wedge. Finally, phase IV (~5-2.4Ma) records two depositional cycles of proximal clastic wedge progradation (FAV) from the southwest (Sierra de Umango) and/or the west (Precordillera). These cycles are represented by coarsening-upward successions from playa lake (FA VI) to braided (FAVII) to piedmonts (FAV) deposits.

Overall in the southern part of the Vinchina basin the Toro Negro Formation presents an initial fining upward column, a thick intermediate fine-grained interval and an upper coarsening upward section. This trend represents an initial retrogradational pattern from medial to distal parts of a distributive fluvial system (phase I) followed by a thick aggradational lacustrine interval (phase II) and finally the progradation of a distal (phase III) to proximal clastic wedge (piedmont, phase IV).

The two new U-Pb ages obtained from volcanic zircons confirm the Late Miocene age for the lower member of the Toro Negro Formation and permit correlation between the southern and central parts of the basin. The sedimentation rate calculated for the dated lacustrine-fluvial interval (6.6 to 5.4 Ma) at Quebrada del Yeso is higher than the corresponding one in the Quebrada de La Troya, suggesting a higher subsidence in the southern part of the basin. Accordingly, the lacustrine interval is much thicker (740 m) and the sedimentation rate higher (1.4 mm/yr) in the south than in the central (240 m and 1.25 mm/yr respectively) part of the basin in agreement with the previously proposed southward fining trend based on the facies distribution of the lower member of the Toro Negro Formation (Ciccioli and Marensi, 2012).

Overall, the Vinchina basin is a good example of a closed basin surrounded by the Precordillera fold and thrust belt to the west and basement-cored blocks to the north, south (Western Sierras Pampeanas) and east (Sierra de Famatina). During the Late Miocene (~7-6.6 Ma) the ephemeral drainage was controlled by an arid to semiarid climate and initially dissipated mostly internally as terminal fan/distributive fluvial systems descending from the north (Sierra de Toro Negro). A thick lacustrine interval developed in the southern part of the basin between ~6.6 and 6.1 Ma during a period of high subsidence and closed drainage favored by the incipient uplift of the Sierra de Umango. Besides, this interval coincides with increased aridity recorded in other basins in the Northwest of Argentina. By the ~6.1 Ma the area started to receive the first coarse-grained sediments heralding the progradation of a clastic wedge from the west-southwest (Precordillera and Sierra de Umango) which fully developed during the rest of the Pliocene to the earliest Pleistocene (~2.4 Ma). This last interval records ameliorating climatic conditions with more moisture.

ACKNOWLEDGEMENTS

The authors appreciate the comments and suggestions provided by two anonymous reviewers and the Regional Editor (V.A. Ramos). This research was supported by Universidad de Buenos Aires (UBACyT GC-385BA), ANPCyT (PICT 2014-1963 and 2015-2239) and CONICET (PIP 262-2015).

REFERENCES

- Amidon, W.A., Ciccioli, P.L., Marensi, S.A., Limarino, C.O., Burch Fisher, G., Burbank, D., Kylander-Clark, A., 2016. U-Pb ages of detrital and volcanic zircons of the Toro Negro Formation, northwestern Argentina: age, provenance and sedimentation rates. *Journal of South American Earth Sciences*, 70, 237-250.
- Amidon, W.A., Burch Fisher, G., Burbank, D.W., Ciccioli, P.L., Alonso, R.N., Gorin, A., Silverhart, P., Kylander-Clark, A.R.C., Christoffersen, M., 2017. Mio-Pliocene aridity in the south-central Andes associated with Southern hemisphere cold periods. *Proceedings of the National Academy of Sciences*, 114(25), 6474–6479.
- Arenas, C., Pardo, G., 1999. Latest Oligocene–Late Miocene lacustrine systems of the north-central part of the Ebro Basin (Spain): sedimentary facies model and palaeogeographic synthesis. *Palaeogeography, Palaeoclimatology, Palaeoecology*, 151(1), 127-148.
- Bentham, P.A., Talling, P.J., Burbank, D.W., 1993. Braided stream and flood-plain deposition in a rapidly aggrading basin: the Escanilla Formation, Spanish Pyrenees. In: Best, J.L. and Bristow, C.S. (Eds.), *Braided Rivers*, Geological Society of London. Spec. Publ., 75, 177-194.
- Bohacs, K.M., Carroll, A.R., Neal, J.E., Mankiewicz, P.J., 2000. Lake basin type, source potential and hydrocarbon character: an integrated sequence-stratigraphic-geochemical framework. In: Gierlowski-Kordesch, E.H., Kelts, K.R. (Eds.), *Lake basins through space and time*. American Association of Petroleum Geologists Studies in Geology, 46, 3–34.
- Bristow, C.S., Skelly, R.L., Ethridge, F.G., 1999. Crevasse splays from the rapidly aggrading, sand-bed, braided Niobrara River, Nebraska: effect of base-level rise. *Sedimentology*, 46, 1029-1047.
- Bywater-Reyes, S., Carrapa, B., Clementz, M., Schoenbohm L., 2010. Effect of late Cenozoic aridification on sedimentation in the Eastern Cordillera of northwest Argentina (Angastaco Basin). *Geology (Boulder)*, 38, 235–238.

- Cain, S.A., Mountney, N.P., 2009. Spatial and temporal evolution of a terminal fluvial fan system: the Permian Organ Rock Formation, South-east Utah, USA. *Sedimentology*, 56, 1774-1800.
- Carrapa, B., Hauer, J., Schoenbohm, L., Strecker, M.R., Schmitt, A.K., Villanueva, A., Gomez, J.S., 2008. Dynamics of deformation and sedimentation in the northern Sierras Pampeanas: An integrated study of the Neogene Fiambala basin, NW Argentina. *Geological Society of America Bulletin*, 120(11-12), 1518-1543.
- Carroll, A.R., Bohacs, K.M., 1999. Stratigraphic classification of ancient lakes: Balancing tectonic and climatic controls. *Geology*, 27 (2), 99–102.
- Ciccioli, P.L., 2008. Evolución paleoambiental, estratigrafía y petrología sedimentaria de la Formación Toro Negro (Neógeno), Sierras Pampeanas Noroccidentales (Provincia de La Rioja). Ph.D. Thesis, Facultad de Ciencias Exactas y Naturales, Universidad de Buenos Aires, Argentina.
- Ciccioli P.L., Marensi, S.A., 2012. Paleoambientes sedimentarios de la Formación Toro Negro (Neógeno), antepaís fracturado andino, noroeste argentino. *Andean Geology*, 39(3), 406–440.
- Ciccioli, P.L., Limarino, C.O., Marensi, S.A., 2005. Nuevas edades radimétricas para la Formación Toro Negro en la Sierra de Los Colorados, Sierras Pampeanas Noroccidentales, provincia de La Rioja. *Revista de la Asociación Geológica Argentina*, 60, 251–254.
- Ciccioli, P.L., Limarino, C.O., Marensi, S.A., Tedesco, A.M., Tripaldi, A., 2010a. Estratigrafía de la cuenca de vinchina (Terciario), sierras pampeanas, provincia de la Rioja. *Revista de la Asociación Geológica Argentina*, 66(1), 146-155.
- Ciccioli, P.L., Limarino, C.O., Marensi, S.A., 2010b. The Vinchina Broken- Foreland Basin: Tectonic Controls in the evolution of the fluvial systems of the Toro Negro Formation (Neogene), NW Argentina. 18th International Sedimentology Congress, Mendoza, Argentina, Abstract, 248.

- Ciccioli, P.L., Limarino, C.O., Marensi, S.A., Tedesco, A.M., Tripaldi, A., 2011. Tectosedimentary evolution of the La Troya-Vinchina depocenters (northern Bermejo Basin, Tertiary), La Rioja Province, Argentina. In: Salfity, J.A., Marquillas, R.A. (Eds.), *Cenozoic Geology of the Central Andes of Argentina*, SCS Publisher, Salta, pp. 91–110.
- Ciccioli, P.L., Marensi, S.A., Limarino, C.O., 2012. Sedimentación de baja energía en la cuenca de Vinchina: el perfil del Miembro inferior de la Formación Toro Negro (Mioceno) en la quebrada del Yeso, La Rioja. 13th Reunión Argentina de Sedimentología, Salta. Resúmenes, 51-52
- Ciccioli, P.L., Marensi, S.A., Rossello, E., Limarino, C.O., 2013a. Sedimentary patterns in the Vinchina Basin: interplay between compressional and transcurrent tectonism during the Andean Orogeny. *Bollettino di Geofisica teorica ed applicata*, 54 S2, 217-220.
- Ciccioli, P.L., Gómez O'Connell, M., Limarino, C.O., Marensi, S.A., 2013b. La sucesión terciaria de la quebrada de Los Pozuelos (Cuenca de Vinchina): su importancia estratigráfica y paleogeográfica para el antepaís andino. *Revista de la Asociación Geológica Argentina*, 70 (4), 451–464.
- Ciccioli, P.L., Marensi, S.A., Limarino, C.O., 2014. Petrology and provenance of the Toro Negro Formation (Neogene) of the Vinchina broken foreland basin (Central Andes of Argentina). *Journal of South American Earth Sciences*, 49, 15–38.
- Ciccioli, P.L., Ré, G.H., Amidon, W.H., Marensi, S.A., Limarino, C.O., 2017. Cronología depositacional de la Formación Toro Negro antepaís andino, La Rioja. 4th Simposio Mioceno-Pleistoceno del Centro y Norte de Argentina. 20th Congreso Geológico Argentino, San Miguel de Tucumán, 31-36.
- Dickinson, W.R., 1988. Provenance and sediment dispersal in relation to paleotectonics and paleogeography of sedimentary basins. In: Kleinspehn, K.L. and Paola C. (Eds.), *New Perspectives in Basin Analysis*. Springer-Verlag, pp. 3 – 25.
- Fisher, J.A., Nichols, G.J., Waltham, D.A., 2007. Unconfined flow deposits in distal sectors of fluvial distributary systems: Examples from the Miocene Luna and Huesca Systems, northern Spain. *Sedimentary Geology*, 195, 55-73.

- Fisher, J.A., Krapf, C.B.E., Lang, S.C., Nichols, G.J., Payenber, T.H.D., 2008. Sedimentology and architecture of the Douglas Creek terminal splay, Lake Eyre, central Australia. *Sedimentology*, 55, 1915–1930.
- Foley, M.G., 1978. Scour and fill in steep, sand-bed ephemeral streams. *Geological Society of America Bulletin*, 89, 559-570.
- Folk, R.L., 1962. Spectral subdivision of limestone types. In: Ham, W.E. (Ed.) *Classification of Carbonate Rocks - A Symposium: American Association of Petroleum Geologists Memoir*, 1, 62-84.
- Gierlowski-Kordesch, E.H., 2010. Lacustrine carbonates. In: Alonso-Zarza, A.M., Tanner, L.H. (Eds.), *Carbonates in Continental Settings: Facies, Environments and Processes. Developments in Sedimentology*, 62, pp. 1-70.
- Hampton, B.A., Horton, B.K., 2007. Sheetflow fluvial processes in a rapidly subsiding basin, Altiplano plateau, Bolivia. *Sedimentology*, 54 (5), 1121–1148.
- Handford, C.R., 1982. Sedimentology and evaporite genesis in a Holocene continental-sabkha playa basin- Bristol Dry Lake, California. *Sedimentology*, 29, 239-253.
- Hardie, L.A., Smoot, J.R., Eugster, H.P., 1978. Saline lakes and their deposits: a sedimentological approach. In: Matter A. and Tucker, M.E. (Eds): *Modern and Ancient Lake Sediments. Special Publication International Association of Sedimentology*, 2, 7-42.
- Hartley, A.J., Weissmann, G.S., Nichols, G.J., Warwick, G.L., 2010. Large distributive fluvial systems: Characteristics, distribution, and control on development. *Journal of Sedimentary Research*, 80, 167–183.
- Hynek, S.A., Passey, B.H., Prado, J.L., Brown, F.H., Cerling, T.E., Quade, J., 2012. Small mammal carbon isotope ecology across the Miocene- Pliocene boundary, northwestern Argentina. *Earth Planetary Science Letter*, 321-322, 177–188.
- Introcaso, A., Ruiz, F., 2001. Geophysical indicators of strike-slip faulting in Desaguadero Bermejo tectonic lineament (northwestern Argentina). *Journal of South American Earth Science*, 14(7), 655-663.

- Jackson, S.E., Pearson, N.J., Griffin, W.L., Belousova, E.A., 2004. The application of laser ablation-inductively coupled plasma-mass spectrometry to in situ U-Pb zircon geochronology. *Chemical Geology*, 211 (1–2), 47–69.
- Japas, M.S., Ré, G.H., Oriolo, S., Vilas J.F., 2016. Basement-involved deformation overprinting thin-skinned deformation in the Pampean flat-slab segment of the southern Central Andes, Argentina. *Geological Magazine*, 153(5/6), 1042–1065.
- Jones, H.L., Hajek, E.A., 2007. Characterizing avulsion stratigraphy in ancient alluvial deposits. *Sedimentary Geology*, 202, 124–137.
- Kelly, S.B., Olsen, H., 1993. Terminal fans - a review with reference to Devonian examples. *Sedimentary Geology*, 85, 339–374.
- Kowalewska, A., Cohen, A.S., 1998. Reconstruction of paleoenvironments of the Great Salt Lake Basin during the late Cenozoic. *Journal of Paleolimnology*, 20(4), 381–407.
- Kraus, M.J., Wells, T.M., 1999. Recognizing avulsion deposits in the ancient stratigraphical record. *Special Publication IAS*, 28, 251–268.
- Kylander-Clark, A.R.C., Hacker, B.R., Cottle, J.M., 2013. Laser ablation split stream ICP petrochronology. *Chemical Geology*, 345, 99–112.
- Limarino, C.O., Tripaldi, A., Marensi, S.A., Net, L.I., Re, G., Caselli, A.T., 2001. Tectonic control on the evolution of the fluvial systems of the Vinchina Formation (Miocene), Northwestern Argentina. *Journal of South American Earth Sciences*, 14(7), 751–762.
- Limarino, C.O., Ciccioli, P.L., Marensi, S.A., 2010. Análisis del contacto entre las formaciones Vinchina y Toro Negro (Sierra de Los Colorados, provincia de La Rioja, Argentina), sus implicancias tectónicas. *Latin American Journal of Sedimentology and Basin Analysis*, 17(2), 113–132.
- Ludwig, K.R., 1991. ISOPLOT; a plotting and regression program for radiogenic-isotope data; version 2.53: Open-File Report - U. S. Geological Survey, p. 39.
- Makaske, B., Smith, D.G., Berendsen, H.J.A., 2002. Avulsions, channel evolution and floodplain sedimentation rates of the anastomosing upper Columbia River, British Columbia, Canada. *Sedimentology*, 49, 1049–1071.

- Malizia, D.C., Reynolds, J.H., Tabbutt, K.D., 1995. Chronology of Neogene sedimentation, stratigraphy, and tectonism in the Campo de Talampaya region, La Rioja Province, Argentina. *Sedimentary Geology*, 96, 231-255.
- Marensi, S.A., Ciccioli, P.L., Limarino, C.O., Schencman, L.J., Díaz, M.Y., 2015. Using fluvial cyclicity to decipher the interaction of basement- and fold-thrust-belt tectonics in a broken foreland basin; Vinchina Formation (Miocene), northwestern Argentina. *Journal of Sedimentary Research*, 85(4), 361–380.
- Mather, A., 2007. Arid environments. In: *Environmental Sedimentology*. Perry C. and Taylor K. (Eds.). Blackwell Publishing, Cap 5, 144-189.
- May, G., Hartley, A.J., Stuart, F.M., Chong, G., 1999. Tectonic signatures in arid continental basins: an example from the Upper Miocene–Pleistocene, Calama Basin, Andean forearc, northern Chile. *Palaeogeography, Palaeoclimatology, Palaeoecology*, 151, 55–77.
- McKie, T., 2014. Climatic and tectonic controls on Triassic dryland terminal fluvial system architecture, central North Sea. In: A.W. Martinius, R. Ravnas, J.A. Howell, R.J. Steel, and J.P. Wonham (Eds.), *From Depositional Systems to Sedimentary Successions on the Norwegian Continental Margin*, First Edition, IAS Special Publication, 46, 19–58.
- Miall, A.D., 1996. *The geology of fluvial deposits*. Springer, 582 pp.
- Nichols, G.J., 2004. Sedimentation and base level controls in an endorheic basin: the Tertiary of the Ebro Basin, Spain. *Boletín Geológico y Minero España*, 115, 427–438.
- Nichols, G.J., 2007. Fluvial systems in desiccating endorheic basins. In: Nichols, G., Williams, E., Paola, C. (Eds.), *Sedimentary Processes, Environments and Basins: A Tribute to Peter Friend*. IAS Special Publication, 38, 569-589.
- Nichols, G.J., Fisher, J.A., 2007. Processes, facies and architecture of fluvial distributary system deposits. *Sedimentary Geology*, 195, 75-90.
- North, C.P., Warwick, G.L., 2007. Fluvial fans: myths, misconceptions, and the end of the terminal-fan model. *Journal of Sedimentary Research*, 77, 693-701.

- Owen, A., Nichols, G.J., Hartley, A.J., Weissmann, G.S., 2017. Vertical trends within the prograding Salt Wash distributive fluvial system, SW United States. *Basin Research*, 29, 64–80.
- Picard, M.D., High, L.R., 1973. Sedimentary structures of ephemeral streams. *Developments in Sedimentology*, 17, 223pp.
- Pietras, J.T., Carroll, A.R., Rhodes, M.K., 2003. Lake basin response to tectonic drainage diversion: Eocene Green River Formation, Wyoming. *Journal of Paleolimnology*, 30(2), 115-125.
- Pietras, J.T., Carroll, A.R., 2006. High-resolution stratigraphy of an underfilled lake basin: Wilkins Paek Member, Eocene Green River Formation, Wyoming, U.S.A. *Journal of Sedimentary Research*, 76, 1197–1214.
- Ramos, V.A., 1970. Estratigrafía y estructura del Terciario en la Sierra de los Colorados (Provincia de La Rioja), República Argentina. *Revista de la Asociación Geológica Argentina*, 25 (3), 359-382.
- Ramos, V.A, Cristallini, E.C., Pérez, D.J., 2002. The Pampean flat-slab of the Central Andes. *Journal of South American Earth Sciences*, 15(1), 59-78.
- Ré, G.H., Barredo, S.P., 1993. Esquema de correlación magnetoestratigráfica de formaciones terciarias aflorantes en las provincias de San Juan, La Rioja y Catamarca. *Revista de la Asociación Geológica Argentina*, 48(3-4), 241-246.
- Reid, I., Frostick, L.E., 1987. Flow dynamics and suspended sediment properties in arid zone flash floods. *Hydrological Processes*, 1, 239-253.
- Retallack, G.J., 2001. *Soils of the Past: An Introduction to Paleopedology*. 2nd edition, Blackwell Science, London.
- Reynolds, J.H., 1987. Chronology of Neogene tectonics in the Central Andean (27° - 33° S) of western Argentina, based on the magnetic polarity stratigraphy of foreland basin sediments, Ph.D. Thesis, Dartmouth College, 353 pp.
- Reynolds, J.H., Jordan, T.E., Johnson, N.M., Damanti, J.F., Tabbutt, K.D., 1990. Neogene deformation of the flat - subduction segment of the Argentine - Chilean Andes:

- Magnetostratigraphic constrains from Las Juntas, La Rioja province, Argentina. Geological Society of America Bulletin, 12, 1607-1622.
- Rossello, E.A., Mozetic, M.E., Cobbold, P.R., de Urreiztieta, M., Gapais, D., 1996. El espolón Umango-Maz y la conjugación sintaxial de los lineamientos Tucumán y Valle Fértil (La Rioja, Argentina). 13th Congreso Geológico Argentino and 3th Congreso de Exploración de Hidrocarburos, Actas 2, 187-194.
- Ruskin, B.G., Jordan, T.E., 2007. Climate change across continental sequence boundaries: paleopedology and lithofacies of Iglesia Basin, Northwestern Argentina. Journal of Sedimentary Research, 77, 661–679.
- Saéz, A., Cabrera, L., Jensen, A., Chong, G., 1999. Late Neogene lacustrine record and palaeogeography in the Quillagua–Llamara basin, Central Andean fore-arc (northern Chile). Palaeogeography, Palaeoclimatology, Palaeoecology, 151, 5–37.
- Saéz, A., Anadón, P., Herrero, M.J., Moscariello, A., 2007. Variable style of transition between Palaeogene fluvial fan and lacustrine systems, southern Pyrenean foreland, NE Spain. Sedimentology, 54, 367–390.
- Schaerer, U., 1984. The effect of initial ^{230}Th disequilibrium on young U-Pb ages; the Makalu case, Himalaya. Earth and Planetary Science Letters, 67(2), 191–204
- Sláma, J., Košler, J., Condon, D.J., Crowley, J.L., Gerdes, A., Hanchar, J.M., Horstwood, M.S.A., Morris, G. A., Nasdala, L., Norberg, N., Schaltegger, U., Schoene, B., Tubrett, M.N., Whitehouse, M.J., 2008. Plešovice zircon - A new natural reference material for U-Pb and Hf isotopic microanalysis. Chemical Geology, 249(1–2), 1–35.
- Slate, J.L., Smith, G.A., Wang, Y., Cerling, T.E., 1996. Carbonate-paleosol genesis in the Pliocene-Pleistocene St. David Formation, southeastern Arizona, Journal of Sedimentary Research, 66 (1), 85-94.
- Smith, G.A., 1986, Coarse-grained nonmarine volcanoclastic sediment: terminology and depositional processes: Geological Society of America Bulletin, 90, 1-10.
- Smith, G.A., 1987a, Sedimentology of volcanism-induced aggradation in fluvial basins: examples from the Pacific Northwest, U.S.A. In: Ethridge, F.G., Flores, R.M., and

- Harvey, M.A. (Eds.), Recent Developments in Fluvial Sedimentology, SEPM Special Publication 39, 217-229.
- Smith, G.A., 1987b. The influence of explosive volcanism on fluvial sedimentation: the Deschutes Formation (Neogene) in central Oregon: *Journal of Sedimentary Petrology*, 57, 613-629.
- Smith, G. A. 2000. Recognition and significance of streamflow-dominated piedmont facies in extensional basins. *Basin Research*, 12, 399-411.
- Sniderman, J.M.K., Woodhead, J.D., Hellstrom, J., Jordan, G.J, Drysdale, R.N., Tyler, J.J., Porch, N., 2016. Pliocene reversal of late Neogene aridification. *Proceedings of the National Academy of Sciences*, 113 (8), 1999-2004.
- Stacey, J.S., Kramers, J.D., 1975. Approximation of Terrestrial Lead Isotope Evolution by a 2-Stage Model. *Earth and Planetary Science Letters*, 26 (2), 207–221.
- Starck, D., Antózegui, L.M., 2001. The late Miocene climatic change –persistence of a climatic signal through the orogenic stratigraphic record in northwestern Argentina. *Journal of South American Earth Sciences*, 14, 763-774.
- Strasser, A., 1986. Ooids in Purbeck Limestones (lowermost Cretaceous) of the Swiss and French Jura. *Sedimentology*, 33, 711-728.
- Tabbutt, K.D., Naeser, Ch.W., Jordan, T.E., Cervený, P.F., 1989. New fission-track ages of Mio-Pliocene tuffs in the Sierras Pampeanas and Precordillera of Argentina. *Revista de la Asociación Geológica Argentina*, 44 (1-4), 408-419.
- Tripaldi, A., Net, L., Limarino, C.O., Marensi, S., Ré, G., Caselli, A., 2001. Paleoambientes sedimentarios y procedencia de la Formación Vinchina, Mioceno, noroeste de la provincia de La Rioja. *Revista de la Asociación Geológica Argentina*, 56(4), 443-465
- Tucker, M.E., 1991. *Sedimentary petrology. An introduction to the origin of Sedimentary Rocks*. Blackwell Scientific Publications, 260 pp., London.
- Turner, J.C.M., 1964. Descripción geológica de la Hoja 15c. Vinchina (Provincia de La Rioja). Dirección Nacional de Geología y Minería. Boletín N° 100, 81pp. Buenos Aires.

- Vessell, R.K., Davies, D.K., 1981. Non-marine sedimentation in an active fore arc basin, In: Ethridge, F.G. and Flores, R.M. (Eds.), Recent and Ancient Nonmarine Depositional Environments: Models for Exploration. SEPM Special Publication, 31, 31-45.
- Warren, J.K., 2016. Evaporites: A Geological Compendium. 2nd edition; revised and expanded, Berlin, Springer, 1807 pp.
- Wiedenbeck, M., Alle, P., Corfu, F., Griffin, W. L., Meier, M., Oberli, F., 1995. Three natural zircon standards for U-Th-Pb, Lu-Hf, trace element and REE analyses. Geostandards Newsletter, 19, 1–23.
- Weissmann, G.S., Hartley, A.J., Nichols, G.J., Scuderi, L.A., Olson, M., Buehler, H., Banteah, R., 2010. Fluvial form in modern continental sedimentary basins: Distributive Fluvial Systems (DFS). *Geology*, 38, 39-42.
- Weissmann, G.S., Hartley, A.J., Scuderi, L.A., Nichols, G.J., Davidson, S.K., Owen, A., Atchley, S.C., Bhattacharyya, P., Chakraborty, T., Ghosh, P., Nordt, L.C., Michel, L., Tabor, N.J., 2013. Prograding distributive fluvial systems - geomorphic models and ancient examples. In: Dreise S.G., Nordt L.C., McCarthy P.L. (Eds.), *New Frontiers in Paleopedology and Terrestrial Paleoclimatology*, SEPM Spec. Pub., 104, 131–147.
- Weissmann, G.S., Hartley, A.J., Scuderi, L.A., Nichols, G.J., Owen, A., Wright, S., Felicia, A.L., Holland, F., Anaya, F.M.L., 2015. Fluvial geomorphic elements in modern sedimentary basins and their potential preservation in the rock record: A review. *Geomorphology*, 250, 187-219.
- Yechieli, Y., Wood, W.W., 2002. Hydrogeologic processes in saline systems: playas, sabkhas, and saline lakes. *Earth-Science Reviews*, 58, 343-365.

FIGURE CAPTIONS

Figure 1. Location of the study area and setting tectonic map where is recognized the Vinchina Basin (VB) and the main morphostructural units: Famatina System, Cordillera Frontal, Precordillera and Northwestern Sierras Pampeanas (1. Sierra de Toro Negro, 2. Sierras

de Umango-Espinal and 3. Sierra de Maz) and the Tucumán (TL) and Valle Fértil-Desaguadero (D-VFL) lineaments.

Figure 2. Geological map of Vinchina Basin showing the location of the studied section.

Figure 3. Boundary surfaces recognized in the Toro Negro Formation (Modified from Miall, 1996).

Figure 4. A. Detail section of the Toro Negro Formation in the southern part of the Sierra de los Colorados (Quebrada del Yeso section) showing the facies associations recognized. B. Facies association map with the distribution of these units.

Figure 5. Schematic diagrams showing lithofacies, bounding surfaces, architecture and interpretation of the facies associations. See Tables 1 and 2 for references.

Figure 6. A. General aspect of FA I; B. Architectural elements of FA I (the numbers represent the boundary surfaces hierarchy, see Fig. 3); C. Intensely bioturbated mudstones (Fmb) of the floodplain of FA I with some bioturbation with meniscus (arrow); D. Contact between FA I and FA II; E. View of FA II showing the dominance of mudstones and coarsening upward cycles; F. Mudstones and gypsum interlaminated (Fl/Fr/El) with intercalations of sandstone tabular bed with planar basal surfaces and wavy tops. G. View of the tuff level (TN43) at the top of the FA II.

Figure 7. A. General view of the fine-grained deposits of FA III; B. Small scale coarsening upward cycles of the FA III. C. Detail of these cycles showing mudstones and gypsum interlaminated (Fl/Fr/El) with sandstones (Sh/Sr); D. Gypsum laminites (El) composed of fibrous crystals with chevron fabric; E. Small-scale ripples preserved at the top of sandstone beds and F. Limestones composed mainly of surficial and spherical ooids.

Figure 8. A. Main architectural elements of FA IV showing abundance of fine deposits (FF and CS) and coal levels (arrow); B. Detail of the floodplain deposits (FF and CS) of FAIV; C. Greenish sandstones (Sm/Sr) with intercalations of thin gypsum laminites (El) of FAIV; D. Mudstones with spheroidal concretions and small coaly wood remains (C, arrow) of FAIV; E. Channel deposits (CHm) with matrix-supported conglomerates

(sandy matrix) and F. Tuff level channelized massive at the base (arrow) and with diffuse stratification at the top. It corresponds to the sample TN 10/07 dated.

Figure 9. A. Architectural element of channel (CHm) of the FA V dominated by GB; B. Polymictic composition of conglomerate clasts of FA V; C. Levels of conglomerate dominated by high-grade metamorphic rocks of FA V; D. Coarsening upward cycles of the FAVI showing the dominance of fine-grained deposits (SHd) and E. Channels CHm) and overbank (SO) deposits of FA VI with fining-upward arrangement.

Fig. 10 A. U-Pb zircon ages from tephra in the Quebrada del Yeso section plotted in descending order of grain age. Error bars show 2s uncertainty. Thick dashed line denotes the preferred age of the tephra, given by the weighted mean of the youngest grain ages that are within 1s uncertainty of each other and B. Inverse concordia plots of the youngest zircon grains used to compute the preferred eruption age. Dashed line shows the best fit isochron anchored at a common $^{207}\text{Pb}/^{206}\text{Pb}$ ratio of 0.84.

Figure 11. Schematic diagram showing the correlation between the Quebrada del Yeso to Quebrada de La Troya sections taking as guide level the tephra samples TN10/07 and Ash8.

Figure 12. Model of evolution of the Toro Negro Formation in the Quebrada del Yeso section.

TABLE CAPTIONS

Table 1. Lithofacies codes for the Toro Negro Formation (Modified from Miall, 1996).

Table 2. Code of architectural elements defined in the Toro Negro Formation (Modified on Miall, 1996 and Fisher et al. 2008).

Table 3. Summary of facies associations recognized in the Toro Negro Formation.

Appendix 1:

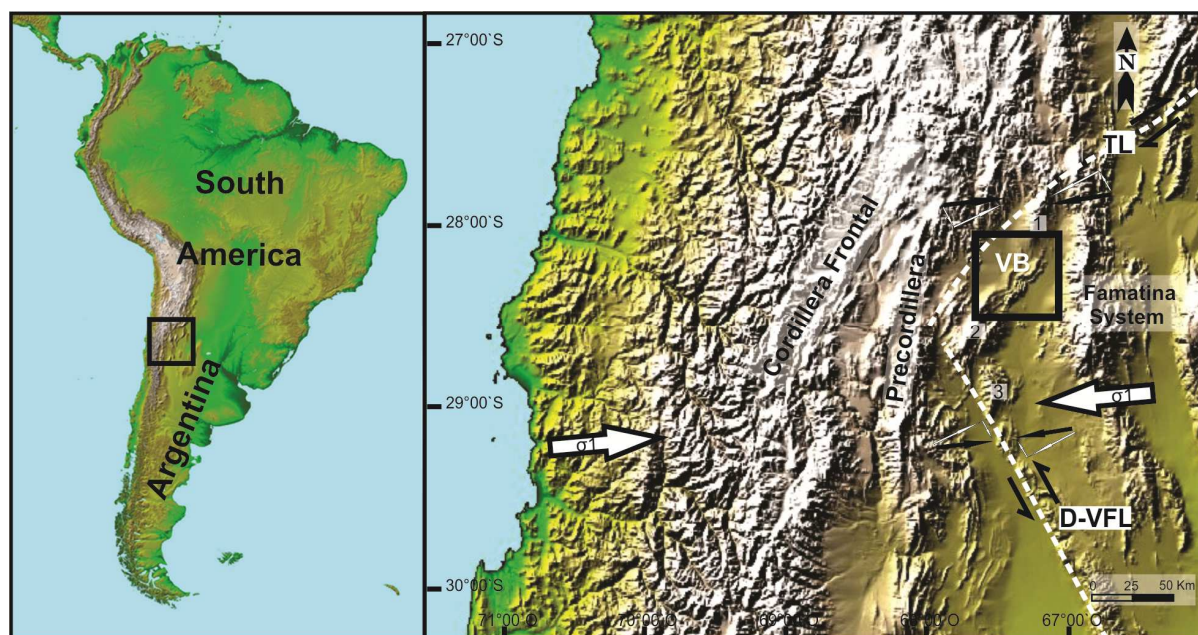
Table S1: U-Pb zircon data from tephra samples.

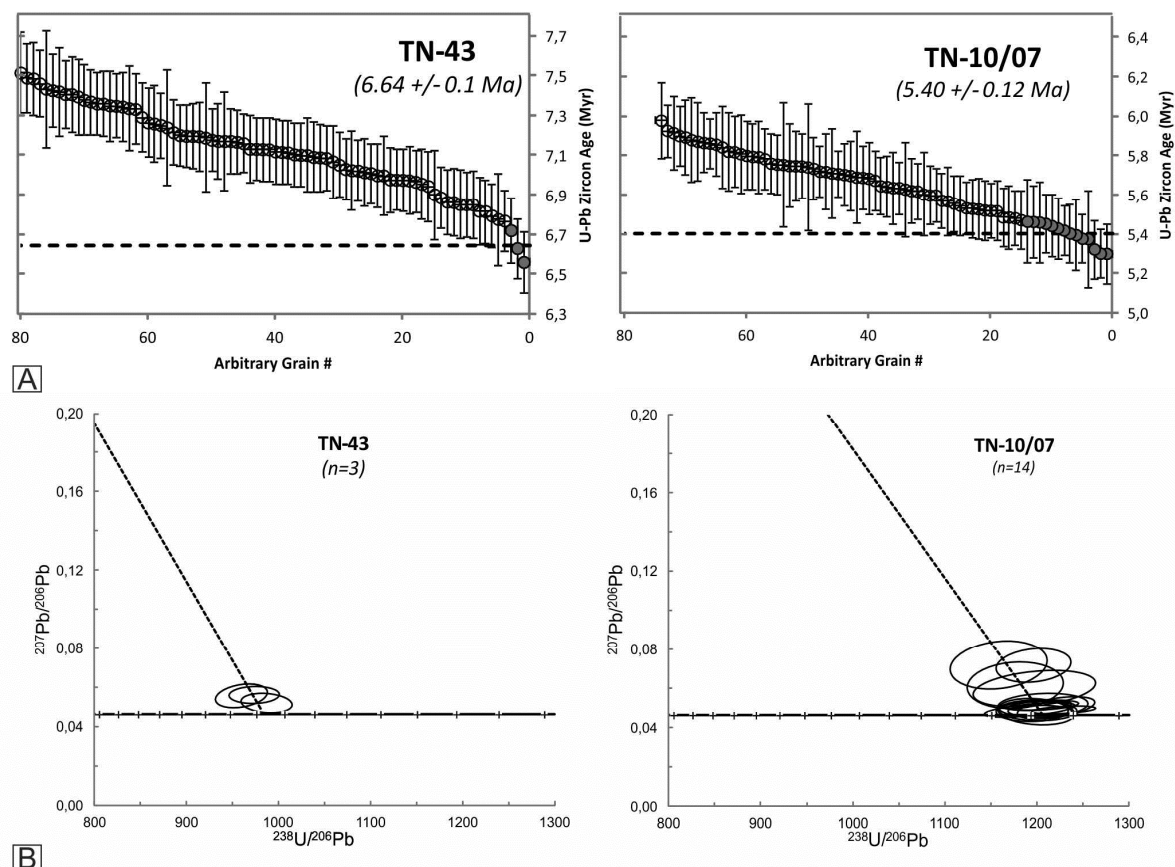
Code	Description of lithofacies
Fl	Horizontal laminated mudstone/siltstone
Fr	Ripple-laminated siltstone
Fm	Massive mudstone/siltstone
El	Horizontal laminated evaporite
Sm	Massive sandstone
She	Heterolithic sandstone
Sr	Ripple-laminated sandstone
Srw	Wave ripple-laminated sandstone
Sh	Horizontal laminated sandstone
Shp	Horizontal laminated sandstone with parting
Sa	Sandstone with antidunes
Sp	Planar cross-bedded sandstone
St	Trough cross-bedded sandstone
Sc	Convolute bedding sandstone
SGm	Massive pebbly sandstone
SGl	Low-angle cross-bedded pebbly sandstone
SGh	Horizontal bedded pebbly sandstone
SGp	Planar cross-bedded pebbly sandstone
SGt	Trough cross-bedded pebbly sandstone
Gm	Masive conglomerate
Gg	Graded conglomerate
Gh	Horizontal bedded conglomerate
Gl	Low-angle cross-bedded conglomerate
Gp	Planar cross-bedded conglomerate
Gt	Trough-cross bedded conglomerate
Gi	Conglomerate with clast imbrication
Gmm	Masive matrix-supported conglomerate
Bi	intraformational breccia

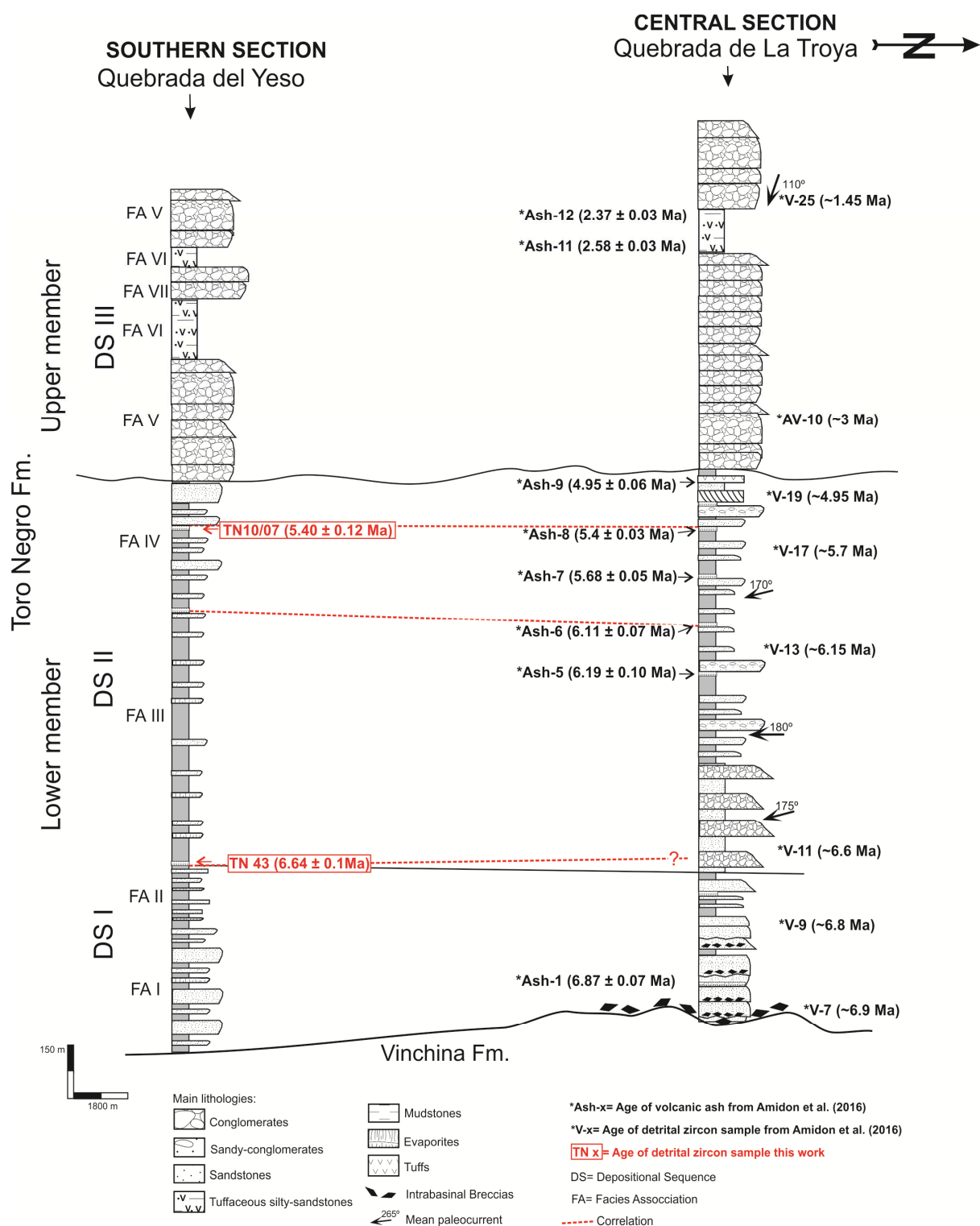
	Code	Architectural element
CHANNEL	CHm	Multistory channel belt
	CHs	Single-story channel
	GB	Gravel bars and bedforms
	SG	Sediment gravity flow element
	SB	Sandy bedform
	DA	Downstream accretion macroform
	LA	Lateral accretion macroform
	LS	Laminated sand sheet
FLOODPLAIN	CR	Crevasse channel
	CS	Crevasse splay
	FF	Overbank fines
	SO	Sandy overbank
	SHp	Proximal splay
	SHd	Distal splay

Table 2. Architectural elements of the Toro Negro Formation.

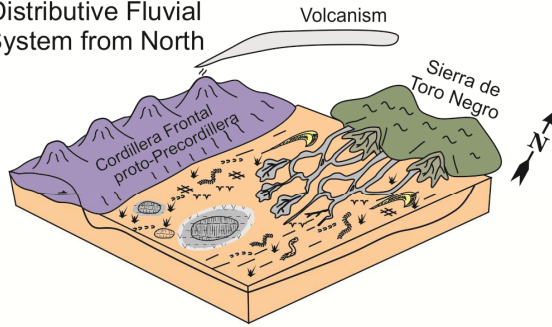
FA	Architectural Elements	Lithofacies	Interpretation
I	CHm, CHs, SB, (LA) FF, CS	Sl, Sh, Shp, She, Sr, Sm, (St, Sp) Fm, Fd El	Shallow sandy fluvial system. Fixed channels flowing over a sandy to mixed sand-mud floodplains.
II	Shp, SHd, FF CHs, SB	Fl, Fr, Fm Sr, Sm, Sh SG m, Gm El	Distal sheetflow-dominated distributive fluvial system. Shallow and ephemeral distributive channels and sheetflows (terminal splays)
III	SH d SH p	Fl, Fr, El She, Sm, Sr, Sh, Shp, Sa L	Mixed clastic-saline, ephemeral lake. Distal sheetfloods. High water table.
IV	FF, CS CHm, GB	Fl, Fr, Fm, Fmc, (El) Sm, Sr, Sl, Sh, Gm, Gp, SGm	Low-sinuosity multichannel river. Sandy to gravelly channels encased in fine-grained floodplains. High aggradation rate.
V	Chm, GB, (SG) SO	Gm, Gi, Gl, Gh, Gp, Gt, (Gmm) SGm, Sm, Sr, (Fm, El)	Streamflow-dominated piedmont.
VI	SH p, SHd, FF CHm, CHs	Sr, Sh, Sm, Sl, (Sc), Fm Bi, Gm, Gi, Gl, Gh, SGm	Mixed sandy-muddy tuffaceous playa-lake with ribbon, shallow gravelly channels
VII	Chm, CHs, GB, SB, (SG) SO, (FF)	Gm, Gt, Gp, Gh, (Gmm) Sm, Sl, Sr, Sh, (Fm, Fr, El)	Deep gravel-bed braided fluvial system. Floodplains dominated by sandy sheetflows.



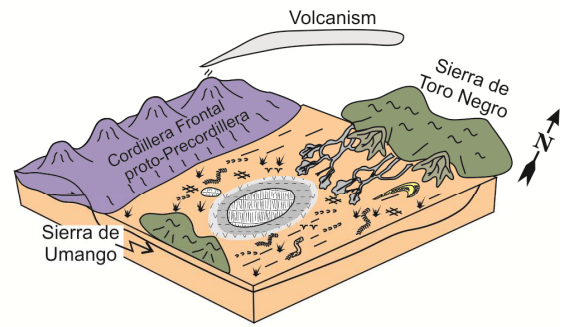




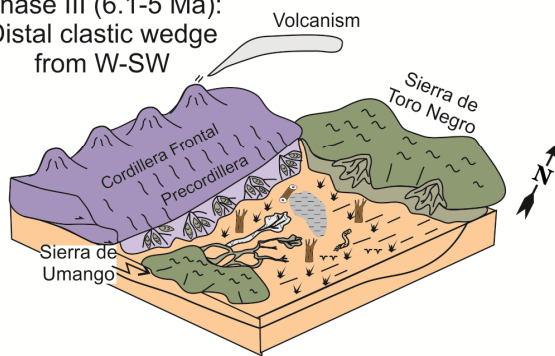
Phase I (7-6.6 Ma):
Distributive Fluvial
System from North



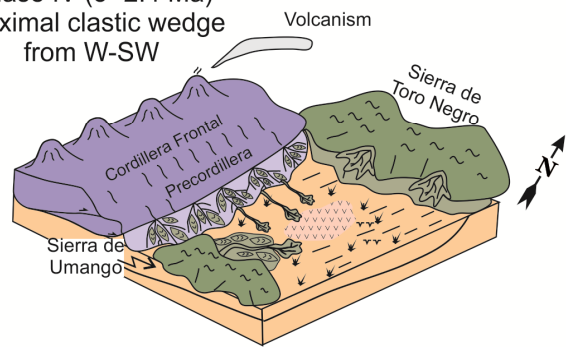
Phase II (6.6-6.1 Ma): ephemeral lacustrine

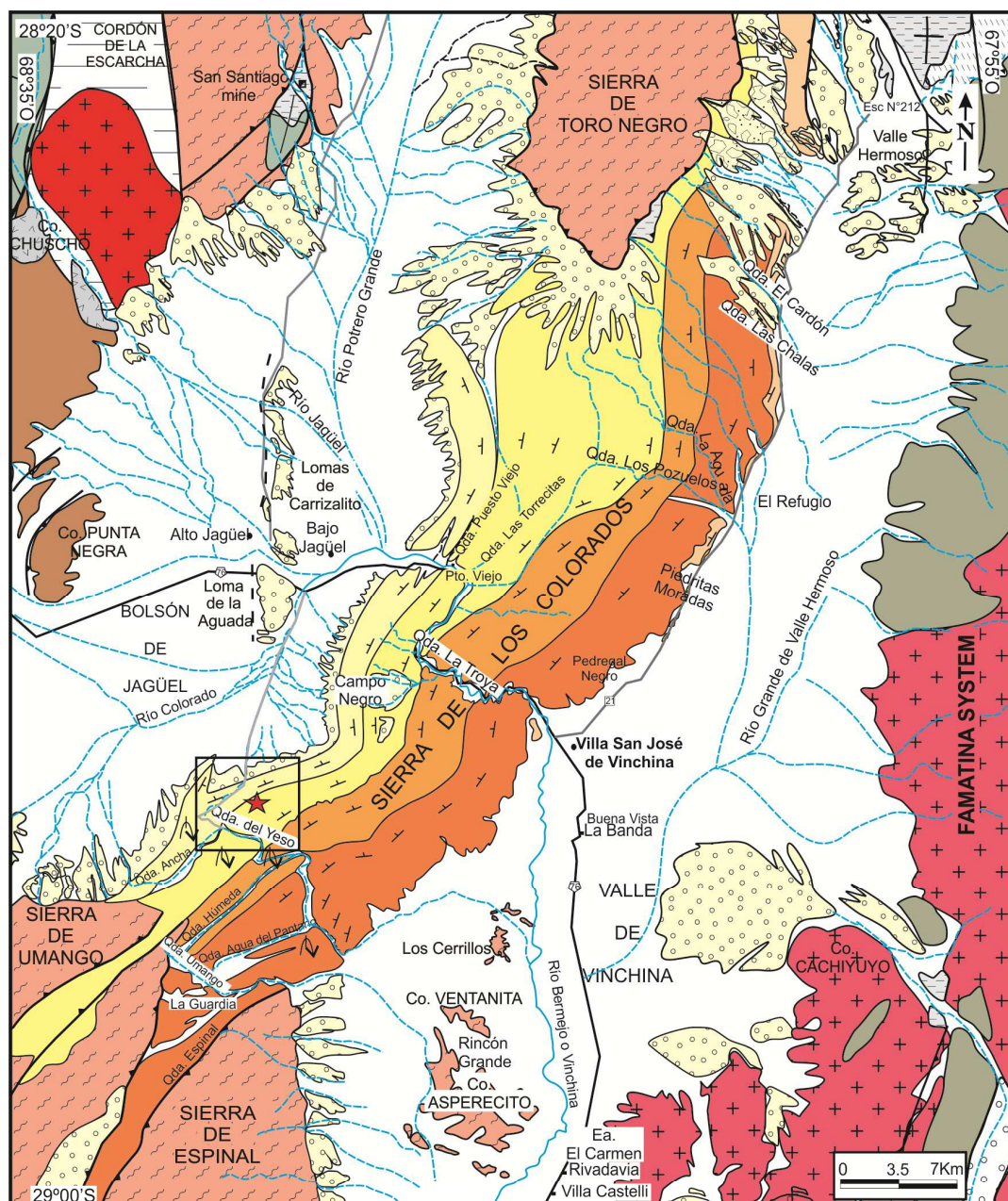


Phase III (6.1-5 Ma):
Distal clastic wedge
from W-SW



Phase IV (5- 2.4 Ma)
Proximal clastic wedge
from W-SW





Cenozoic	Quaternary	Holocene
		Pleistocene
	Neogene	Pliocene
		Miocene
	Paleog.	Oligocene
		Eocene
	Paleozoic	Permian
		Carboniferous
		Devonian
		Ordovician
		Proterozoic

Alluvial, colluvial, and eolian deposits

Pleistocene

El Corral Fm.

Upper Mb.

Lower Mb.

Upper Mb.

Lower Mb.

Vallecito Fm.

Puesto La Flecha Fm.?

De La Cuesta Fm.

Agua Colorada Fm.

Jagüel Fm.

Guacachico/ Nuñorco Fm.

Río Bonete Fm.

Chuscho Fm.

Umango/ Espinal Fm.

Toro Negro Fm.

Vinchina Fm.

Granites

Río del Peñón Fm.

Suri Fm.

Syncline

Anticline

Deformation

Reverse Fault/Thrust

Normal Fault

Inferred Fault

Strike and dip

City

Town

Puesto

Mine



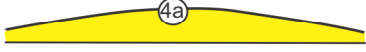





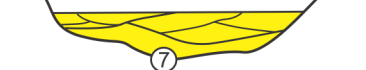
Trackway

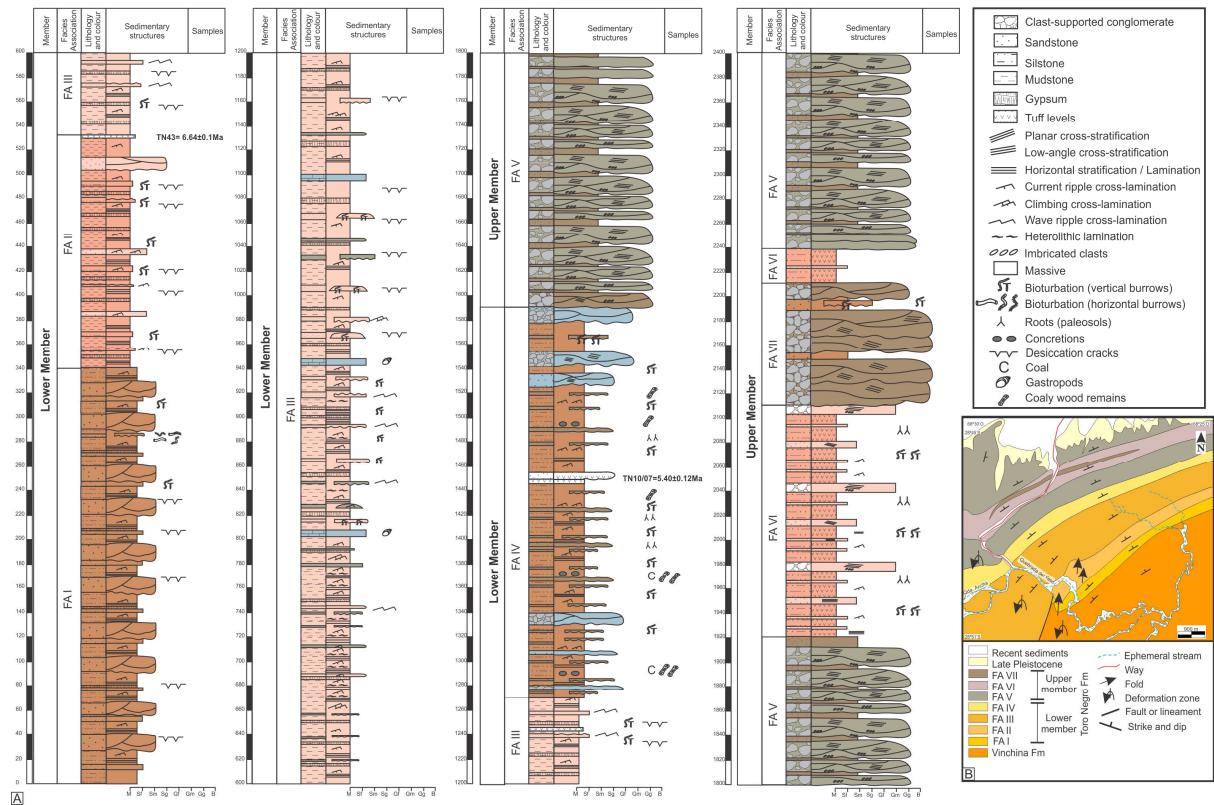
Route

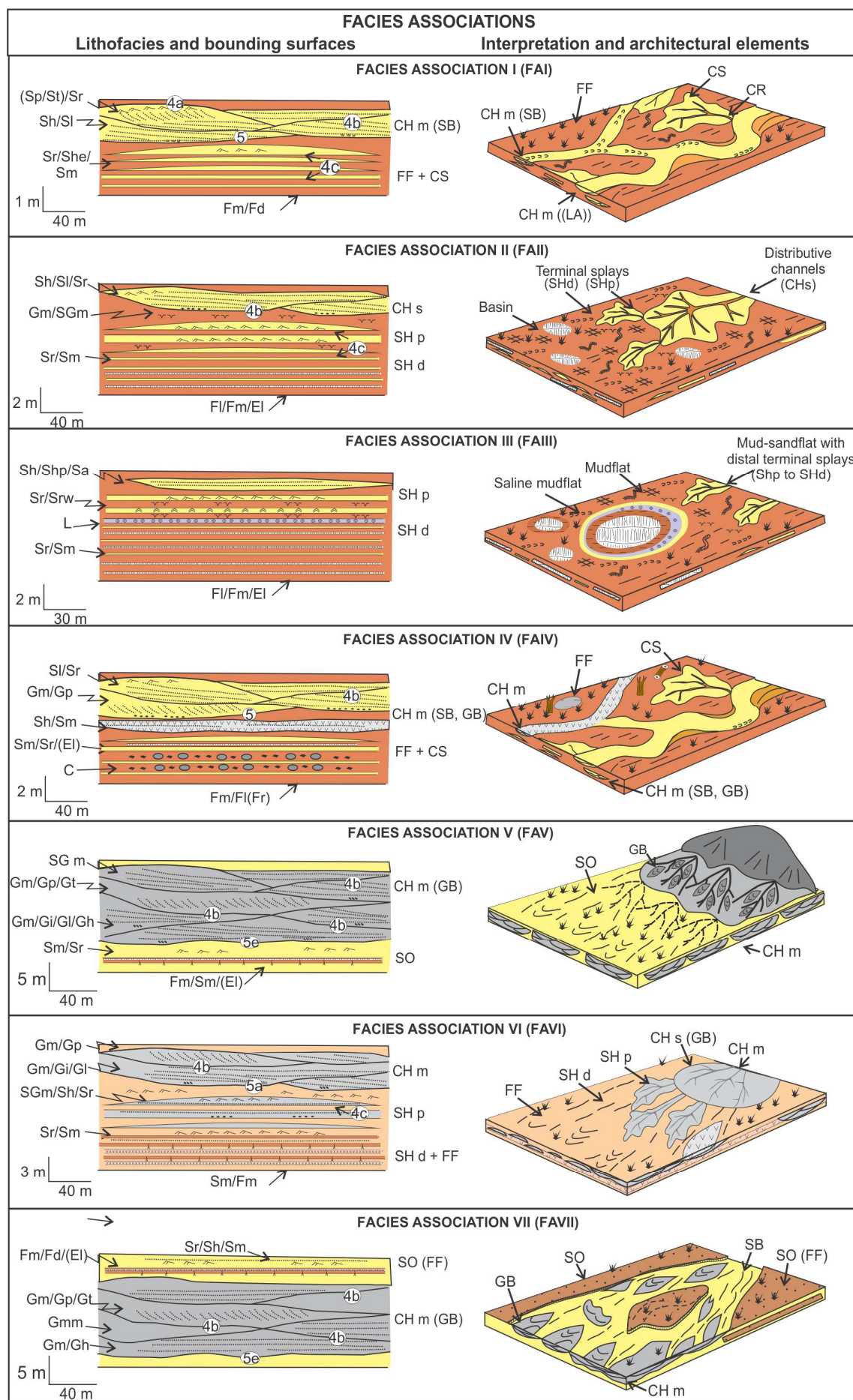
Ephemeral stream

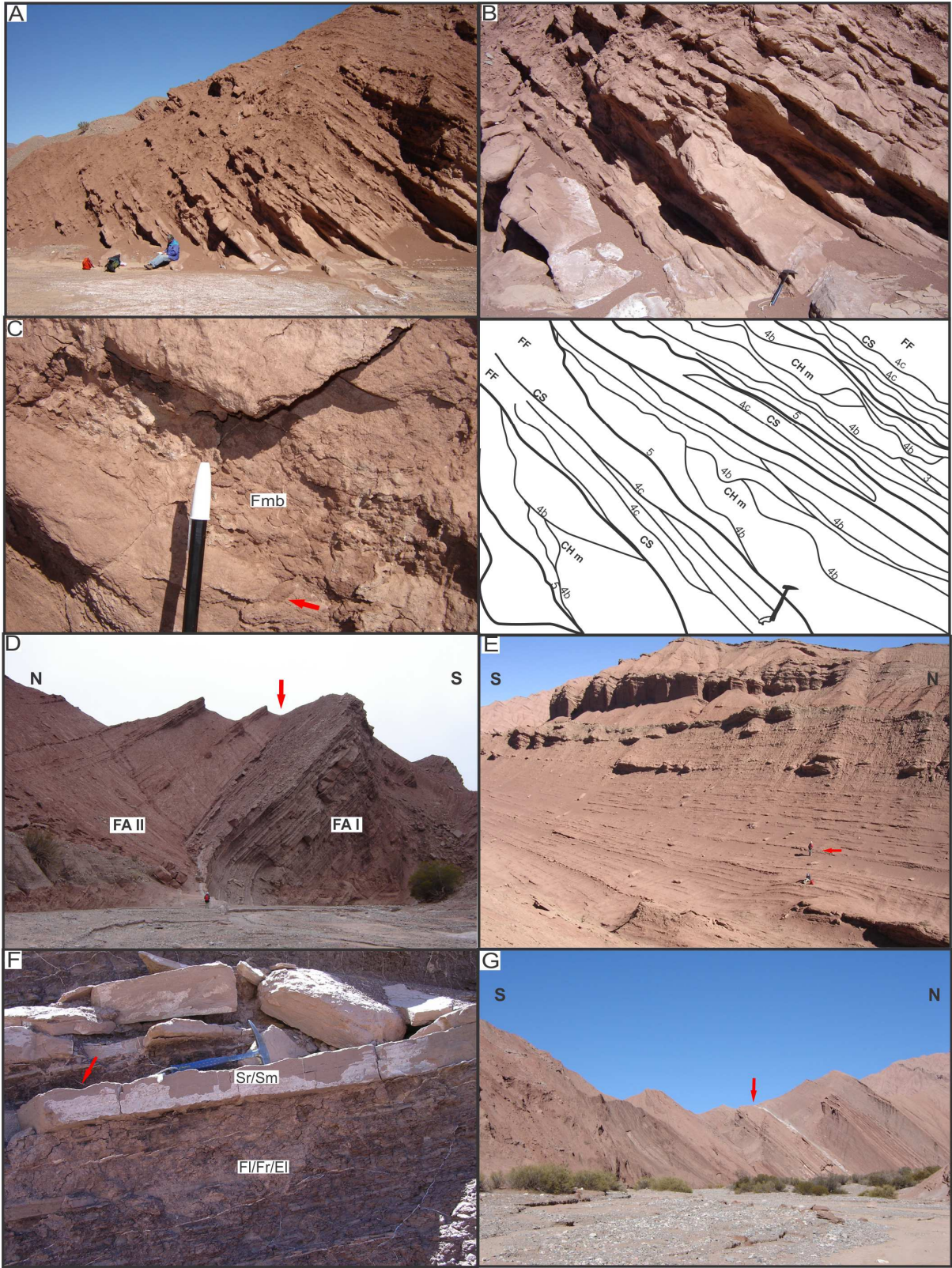
River

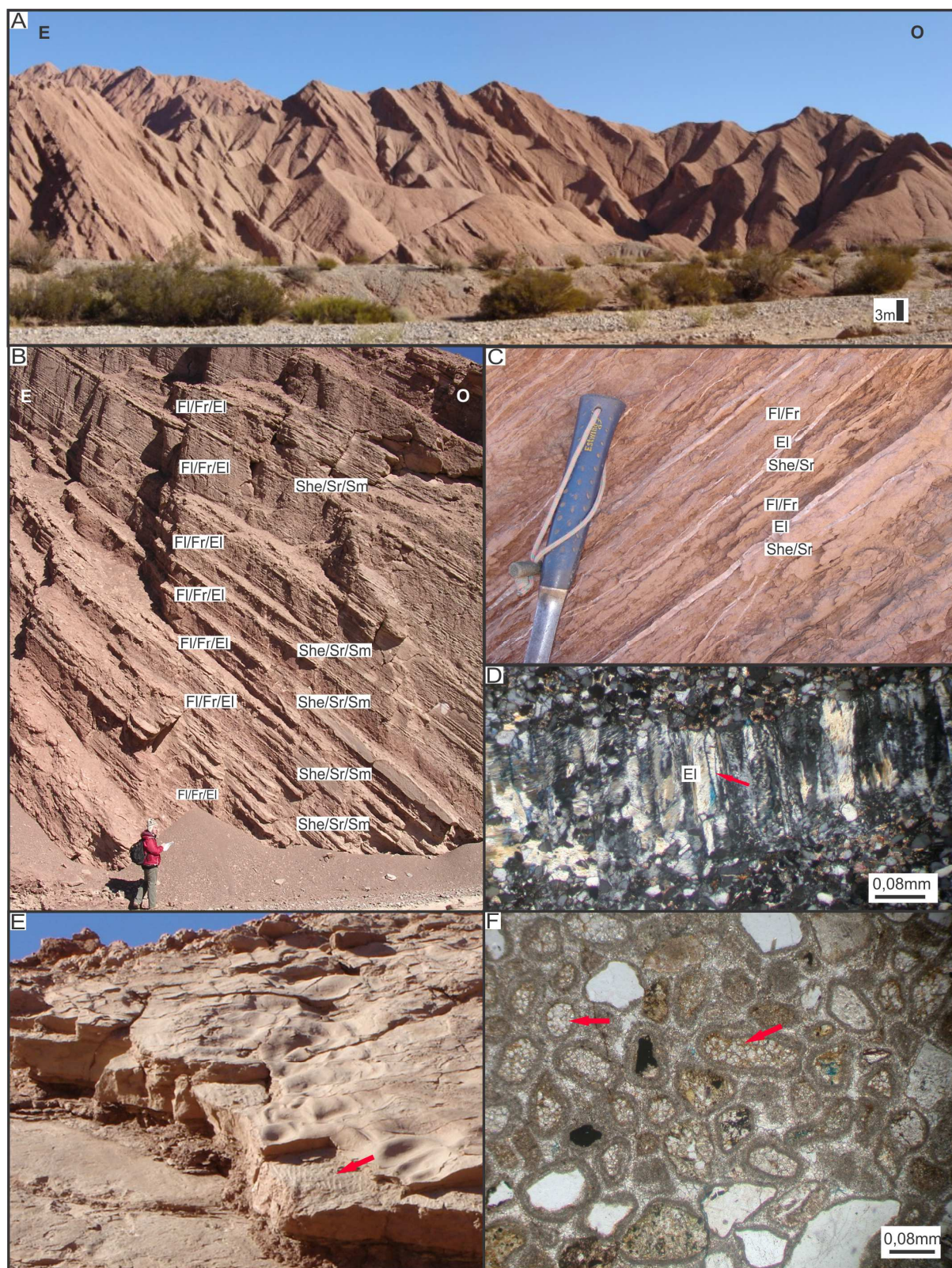
Studied section

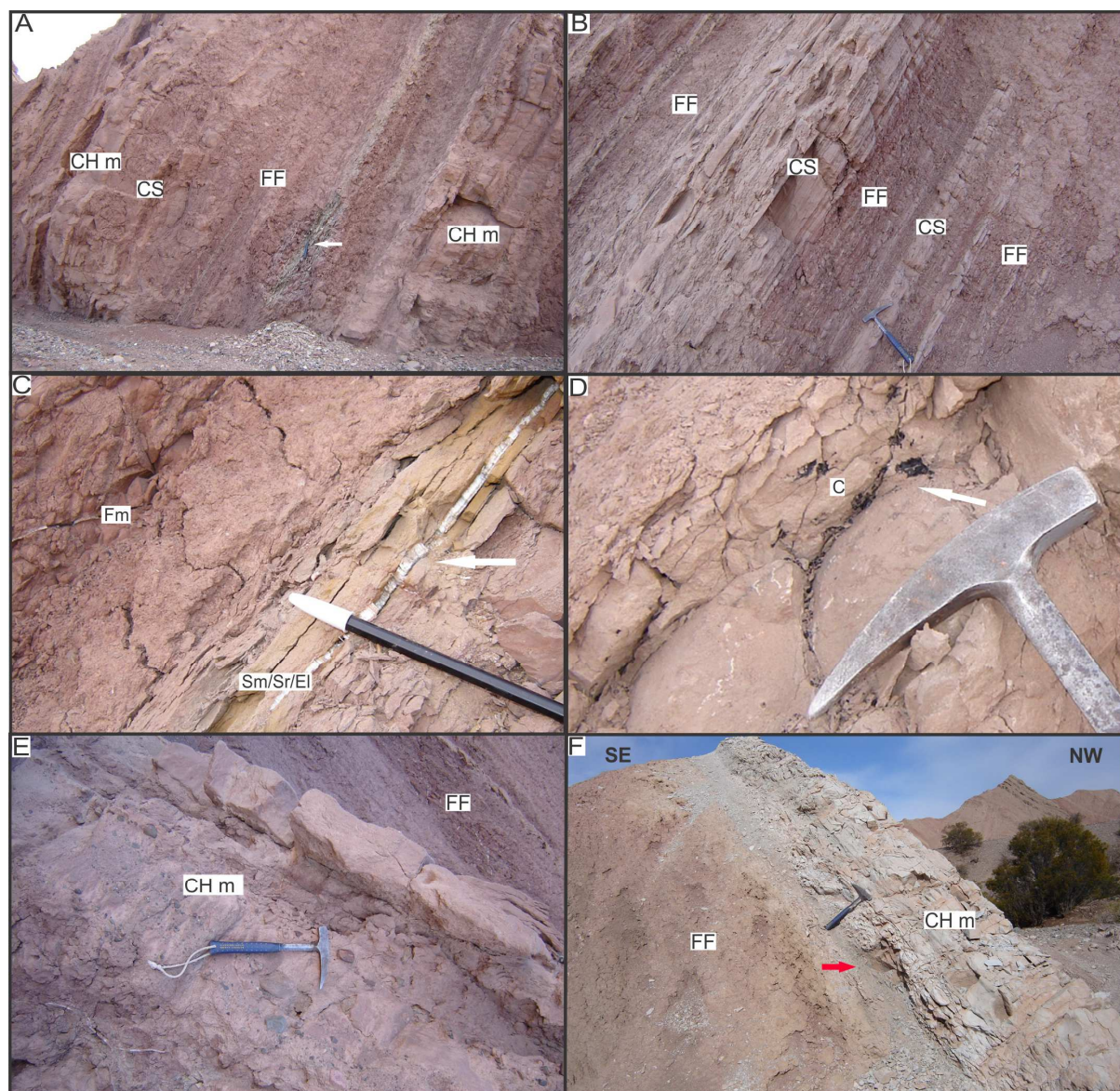
BOUNDING SURFACES		
Order	Architecture	Interpretation
1 st and 2 nd order		Micro and mesoform migration
3 th order		Style bar migration Lateral or down-stream accretion macroform
4 th order		4a: Top of macroform (bar)
		4b: Plane to erosive base of secondary channels (i.e. channel fill complex)
		4c: Plane to convex-up surfaces bounding lithosomes into the floodplain (i.e. crevasse splay)
5 th order		5a: Plane to slightly erosive base of channel complexes
		5e: Strongly erosive surface of channel complexes
6 th order		Low relief large scale incision. Paleovalley of regional extent
7 th order		Major incision surface or paleovalley. Boundary sequence.













We study a 2400 m-thick lacustrine and DFS sequence of the Toro Negro Fm.

Two U-Pb ages of 6.64 ± 0.1 Ma and 5.40 ± 0.12 Ma are present.

We analyze the evolution of an endhoreic basin during the Mio-Pliocene.

We assess the chronology of the Neogene uplift of the Umango range.

We evidence arid conditions during Late Miocene.

An ameliorating climatic condition is recorded to the ~5 Ma.